NON-GAUSSIAN ERROR DISTRIBUTIONS OF ASTROPHYSICAL MEASUREMENTS

by

SARA CRANDALL

B.S., Kansas State University, 2012

A THESIS

submitted in partial fulfillment of the
requirements for the degree

MASTER OF SCIENCE

Department of Physics
College of Arts and Sciences

KANSAS STATE UNIVERSITY
Manhattan, Kansas

2016

Approved by:

Major Professor
Dr. Bharat Ratra

Copyright

Abstract

In physics, datasets are often assumed to follow a Gaussian distribution. However, this may not always be justified. By constructing error distributions, or histograms of the number of standard deviations that a measurement deviates from a central estimate, the Gaussianity of datasets can be explored. This thesis applies statistical techniques used to test the Gaussianity of two datasets.

These techniques are first applied to a ^{7}Li abundance dataset, where error distributions are constructed for 66 measurements (with error bars) used by [1] that give A(Li) $= 2.21 \pm 0.065$ dex (median and 1σ symmetrized error). This error distribution is somewhat non-Gaussian, with large probability in the tails. Assuming Gaussianity, the observed A(Li) is 6.5σ away from that expected from standard Big Bang nucleosynthesis given by *Planck* observations. Accounting for the non-Gaussianity of the observed A(Li) error distribution reduces the discrepancy to 4.9σ, which is still significant.

Similar error distributions are constructed for a compilation of 232 Large Magellanic Cloud (LMC) distance moduli values from [2] that give an LMC distance modulus of $(m - M)_0 = 18.49 \pm 0.13$ mag (median and 1σ symmetrized error). When using a weighted mean (median) central estimate, the error distribution has large (small) probability in the tails than what is expected for a Gaussian distribution. This may be the consequence of publication bias and/or correlations between measurements.

Table of Contents

List of Figures

List of Tables

Acknowledgments

There are many people that helped me successfully complete this thesis. I owe most of my thanks to my advisor, Dr. Bharat Ratra. It is because of you that I have become an independent critical thinker. Thank you for accepting nothing other than published papers from my work. You've given me skills critical for moving on in my career.

I would also like to thank many faculty members at Kansas State. Thank you Dr. Amit Chakrabarti, Dr. Kristan Corwin, and Dr. Mick O'Shea for believing in my abilities and for allowing me to prove myself. Thank you Dr. Vinod Kumarappan and Dr. Lado Samushia for humoring my questions and not kicking me out of your offices. I want to thank Dr. Glenn Horton-Smith and Dr. Andrew Ivanov for answering all of my ROOT questions. I would not have beautiful plots without you. Thank you Dr. Larry Weaver for showing an interest in my education throughout my entire time at K-State. Finally, I want to thank Dr. Tim Bolton for guiding me through the EIDRoP program and for all of your support.

I want to thank Omer Farooq, Anatoly Pavlov, Mikhail Makouski, Saima Farooq, and Sachiko Toda McBride for mentoring me in cosmology, high energy physics, computational physics, and everything else that I needed in order to be a successful graduate student. You are all admirable people, and I look up to you.

The work in this thesis could not have been completed without the help of Stephen Houston, Tia Camarillo, and Jacob Peyton. You are all hard workers and I wish you the best as you pursue your physics/astronomy careers.

I thank M. Spite for providing us with helpful insight and the ^{7}Li abundance compilation. I am also grateful to F. Spite for useful advice. Thank you to R. de Grijs, J. Wicker, and G. Bono for providing us with the LMC distance moduli measurements. In addition, I thank R. de Grijs and J. Wicker for useful comments and advice.

Finally, I want to thank all of my family and friends for supporting me as I pursue my career goals. I especially want to thank my mom, Diana, for being the best friend that I could ask for.

This work was supported in part by DOE Grant No. DEFG 03-99EP41093, and NSF Grant Nos. AST-1109275 and PHY-1157044.

Dedication

To my smart, beautiful, and terribly hardheaded daughter, Tessa.

Chapter 1

Introduction

It is common practice to assume astrophysical datasets to be Gaussian. However, this may not always be justified. By constructing and performing Gaussianity tests on error distributions of measurements, several insights can be gained. These include the possible reduced significance of discrepancies between expected and measured values, the indication that quoted errors might be too optimistic, possible publication biases, or an indication that correlations between measurements may not be as negligible as thought. This thesis explores the statistics needed for this type of analysis in Chapter 1. These techniques are applied to a compilation of ^{7}Li abundance measurements in Chapter 2 and LMC/SMC distance moduli measurements in Chapter 3. Conclusions are presented in Chapter 4.

1.1 Weighted Mean and Median Statistics

Before performing Gaussianity tests on a constructed error distribution, a central estimate must be found. It is popular to do this using either weighted mean or median statistics, and both have different advantages.

Weighted mean statistics makes use of a dataset's quoted errors, and it is conventional when errors are known to be reliably estimated. This method has the advantage in that

a goodness of fit criterion can be used as a diagnostic tool. The standard weighted mean formula for parameter q, as given in [3], is

$$q_{\rm wm} = \frac{\sum_{i=1}^{N} q_i/\sigma_i^2}{\sum_{i=1}^{N} 1/\sigma_i^2}. \tag{1.1}$$

Here, q_i and σ_i are the estimates and one standard deviation errors of $i = 1, 2, ..., N$ measurements, respectively. One can also find the weighted standard deviation given by

$$\sigma_{\rm wm} = \left(\sum_{i=1}^{N} 1/\sigma_i^2 \right)^{-1/2}. \tag{1.2}$$

The goodness of fit, reduced χ^2, is

$$\chi_\nu^2 = \frac{1}{N-1} \sum_{i=1}^{N} \frac{(q_i - q_{\rm wm})^2}{\sigma_i^2}. \tag{1.3}$$

The number of standard deviations that χ_ν deviates from unity, which is also a goodness of fit indicator, is given by

$$N_\sigma = |\chi_\nu - 1| \sqrt{2(N-1)}. \tag{1.4}$$

Large N_σ can be used as an indicator of non-Gaussianity, possibly a consequence of correlations between measurements or unaccounted-for systematic errors.

Median statistics also has advantages. Since this method does not make use of an individual measurement's error, it is a useful tool when using datasets with unknown or poorly estimated errors. Although it has the disadvantage that the error associated with the median will be larger than in the weighted mean case. This method makes fewer assumptions than the weighted mean technique. If one assumes that measurements are statistically independent, and that there is no systematic error for the data as a whole, then as the number of measurements, N, goes to infinity, the median will be revealed as a true value. In this case, the median and weighted mean values should converge. The median is

defined as the value with 50% of the measurements being above it and 50% below. $\sigma_{\rm med}$ is then defined such that the range $q_{\rm med} \pm \sigma_{\rm med}$ includes 68.3% of the probability. For a detailed description of median statistics, see [4].[1]

1.2 Gaussian Distribution

It is conventional within the sciences to assume Gaussianity of a dataset.[2] That is, that data errors have a Gaussian distribution. A Gaussian distribution of data is often described by a bell-shaped curve (see Figure 1.1), and has a probability distribution function of

$$P(x) = \frac{1}{\sqrt{2\pi}} e^{-|x|^2/2}. \tag{1.5}$$

The probabilities of finding a measurement within 1σ, 2σ, and 3σ are 68.3%, 95.4%, and 99.7% respectively (see Figure 1.2).

1.3 Non-Gaussian Distributions

Non-Gaussian distributions are also often used to fit data within physics. Three well-known distributions are described below: the Lorentzian, the Student's t, and the double exponential.

The Lorentzian, or Cauchy, distribution has an extended tail. That is, the tails have greater probability in them than those of a Gaussian. A Lorentzian is thus a popular choice for describing widened distributions. This distribution is described by the probability function

$$P(x) = \frac{1}{\pi} \frac{1}{1 + |x|^2}. \tag{1.6}$$

[1] For other applications and discussions see [5], [6], [7], [8], [9], [10], [11], [12], [13], [14], [15], [16], [17], and [18].

[2] For examples within cosmology see [19, 20, 21, 22]. Here Gaussianity is assumed to constrain data from cosmic microwave background (CMB) anisotropy data. For examples of CMB Gaussianity tests see [23, 24].

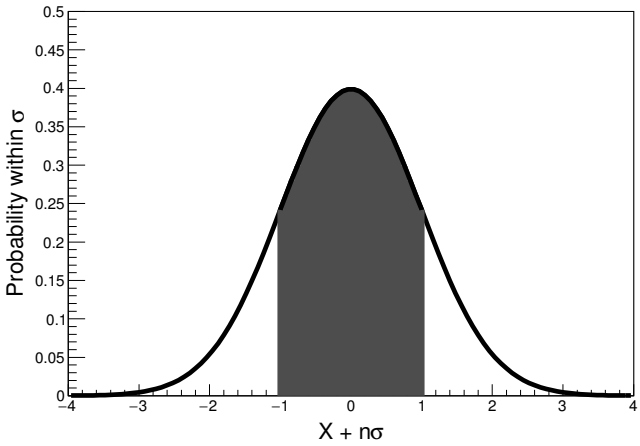

Figure 1.1: *Bell-shaped curved from a Gaussian probability distribution function. The shaded area is the probability of finding a measurement between $X - \sigma$ and $X + \sigma$, where X is the central estimate and n ($n = 1$ here) is the number of standard deviations. In this case, 68.3% is shaded corresponding to 1σ.*

A plot of this distribution can be seen in Figure 1.3. For this distribution, the probabilities of finding a measurement within 1σ and 2σ are 50.0% and 71.0% respectively. Alternatively, 68.3% and 95.4% of measurements fall within 1.8σ and 14.0σ.

The Student's t distribution also has extended tails, but less so than that of a Lorentzian distribution. It is described by the probability distribution function

$$P(x) = \frac{\Gamma[(n+1)/2]}{\sqrt{\pi n}\Gamma(n/2)} \frac{1}{(1+|x|^2/n)^{(n+1)/2}}. \tag{1.7}$$

Here n is a positive, integer parameter and Γ is the gamma function. As $n \to \infty$, the distribution becomes Gaussian, and when $n = 1$ it is a Lorentzian distribution. Varying n will change the expected probabilities for this function. For example, the probabilities of finding a measurement within 1σ and 2σ for an $n = 8$ Student's t distribution are 65.0% and 92.0% respectively. Alternatively, 68.3% and 95.4% of measurements fall within 1.1σ and 2.4σ in this case. This distribution is illustrated in Figure 1.4.

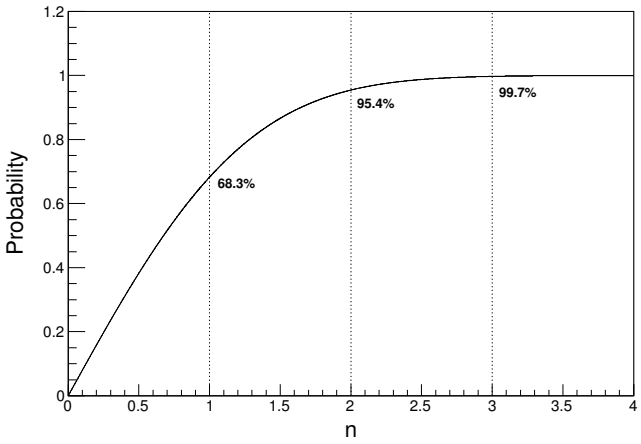

Figure 1.2: *Plot of probabilities given by Gaussian probability distribution function (see Equation 1.5).*

Finally, the Double Exponential (or Laplace) distribution is described by the function

$$P(x) = \frac{1}{2}e^{-|x|}. \tag{1.8}$$

This distribution falls off more rapidly than a Lorentzian, but not as quickly as a Gaussian. For this distribution, the probabilities of finding a measurement within 1σ and 2σ are 63.0% and 87.0% respectively. Alternatively, 68.3% and 95.4% of measurements fall within 1.2σ and 3.1σ. A plot of this distribution can be seen in Figure 1.5.

1.4 N_σ

Determining the Gaussianity of a dataset is an important exercise used to understand the nature of the measurements. Creating an error distribution is one technique used to check how Gaussian a dataset is. Once a central estimate is found, e.g. the median or weighted mean, then an error distribution can be created from N_σ, defined by

$$N_{\sigma_i} = \frac{x_i - x_{\mathrm{CE}}}{(\sigma_i^2 + \sigma_{\mathrm{CE}}^2)^{1/2}}. \tag{1.9}$$

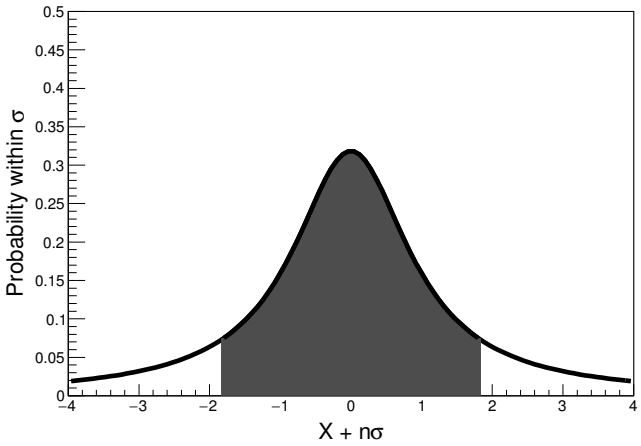

Figure 1.3: *Curve described by a Lorentzian probability distribution function with extended tails. The shaded area is the probability of finding a measurement between* $X - 1.8\sigma$ *and* $X + 1.8\sigma$*, where* X *is the central estimate and* n *(*$n = 1.8$ *here) is the number of standard deviations. In this case, 68.3% is shaded, corresponding to* 1.8σ*.*

Here, x_{CE} is the central estimate with corresponding σ_{CE}, and σ_i is the error associated with each value x_i. The error associated with the central estimate does not necessarily have to be incorporated. There may also be a case where a dataset has non-symmetrical errors. In this case, if $x_i < x_{\mathrm{CE}}$, then

$$N_{\sigma_i} = \frac{x_i - x_{\mathrm{CE}}}{\sigma_i^l}. \tag{1.10}$$

If $x_i > x_{\mathrm{CE}}$ then

$$N_{\sigma_i} = \frac{x_i - x_{\mathrm{CE}}}{\sigma_i^u}. \tag{1.11}$$

Here, σ_i^l and σ_i^u are the lower and upper limit associated errors respectively.

1.5 Methods of Determining Gaussianity

There are several methods used to examine the Gaussianity of a dataset. Two quantifying methods will be outlined in this section.

A goodness of fit test popularly used is the χ^2 analysis. Once N_{σ_i} for each measurement of a dataset is determined, the data is binned. One choice for binning is to follow [25] and

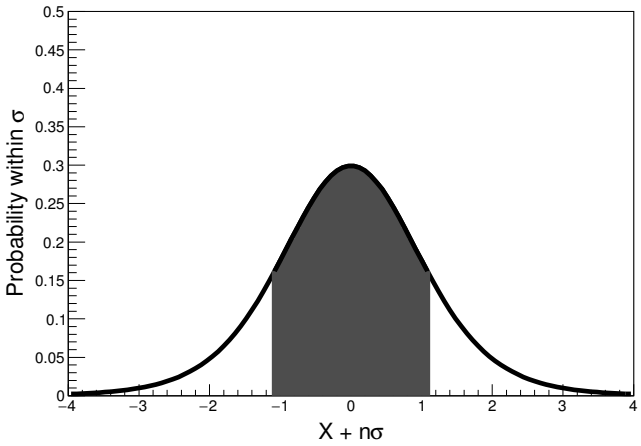

Figure 1.4: *Curve described by an $n = 8$ (n here should not be confused with the n of the standard deviation) Student's t probability distribution function. This distribution has extended tails, but less so than that of a Lorentzian. The shaded area is the probability of finding a measurement between $X - 1.1\sigma$ and $X + 1.1\sigma$, where X is the central estimate and n ($n = 1.1$ here) is the integer number of standard deviations. In this case, the $n = 8$ Student's t distribution has 68.3% shaded, corresponding to 1.1σ.*

bin by the square root of the total number of measurements. This is done in order to both maximize the number of bins and the number of measurements per bin. Bins can be of varying width to ensure equal probability in each bin for an assumed distribution function $P(|N_\sigma|)$.[3] Then using the average $|N_\sigma|$ of each bin to represent the bin as a whole,

$$\chi^2 = \sum_{j=1}^{T} \frac{[M(|N_\sigma|_j) - NP(|N_\sigma|_j)]^2}{NP(|N_\sigma|_i)}. \tag{1.12}$$

Here $M(|N_\sigma|)$ is the number of measurements in each bin, N is the total number of measurements in the dataset, and T is the number of bins. The assumed distribution function can be one of the four mentioned in Sections 1.2 and 1.3: Gaussian, Lorentzian, Student's t, or Double Exponential.

The goodness of fit for each assumed probability distribution is determined by χ^2. That is, a small χ^2 represents a good fit. Furthermore, χ^2 can be minimized by introducing a

[3]For this analysis the absolute N_σ, $|N_\sigma|$ which represents a symmetrical distribution, is used.

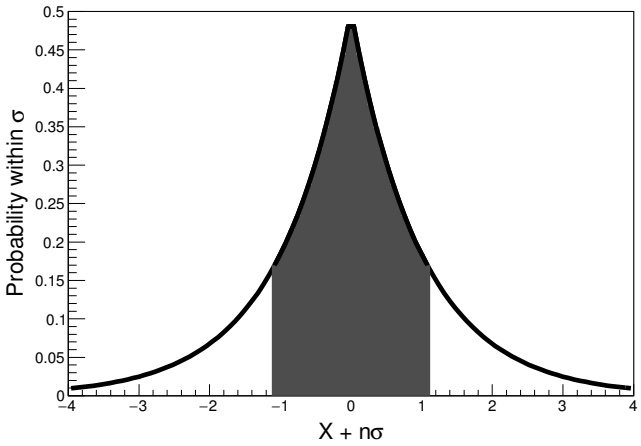

Figure 1.5: *Curve described by a Double Exponential probability distribution function. falls off more rapidly than a Lorentzian, but not as quickly as a Gaussian. The shaded area is the probability of finding a measurement between* $X - 1.2\sigma$ *and* $X + 1.2\sigma$*, where* X *is the central estimate and* n *(*$n = 1.2$ *here) is the number of standard deviations. In this case, 68.3% is shaded, corresponding to* 1.2σ*.*

scale factor S. Thus, $|N_\sigma|/S$ is used to vary the width of a distribution. The reduced χ^2, $\chi^2_\nu = \chi^2/\nu$, is also calculated. Here ν is the number of degrees of freedom that is equal to the number of bins minus one $(T - 1)$. It should be noted that in the case of an assumed Student's t distribution the number of degrees of freedom decreases by one due to the additional parameter n. The scale factor S also introduces another parameter and thus reduces ν by one. Next, one can find the probability that a random sample of data points drawn from the assumed distribution gives a value of χ^2_ν greater than or equal to the observed value.[4] This can be done either numerically or can be found in a Table [see Table 26.7 of 26]. From χ^2_ν and the probability, one is able to quantitatively describe the spread of measurements of a given dataset, and hence makes conclusions about the Gaussianity of said set.

It may also be beneficial to quantify the Gaussianity of a given dataset by using a non-parametric analysis. One method for doing so is to perform a Kolmogorov-Smirnov

[4]For this analysis it is assumed that the bins are uncorrelated, which may not necessarily be true. Therefore, it is more valuable to put more quantitative emphasis on χ^2_ν rather than the probability.

(KS) test. The output (p-value) of this test gives the probability that a given distribution is compatible with a reference distribution. This test can be done using either binned or un-binned data, although it is often argued that un-binned data is more appropriate (see Section 5.3.1 of [27]).

Chapter 2

Non-Gaussian Error Distribution of ^{7}Lithium Abundance Measurements

This chapter explores the discrepancy between expected and observed ^{7}Li abundance measurements found in stars formed from primordial clouds. This discrepancy is known as the "lithium problem." Here, non-Gaussianity of the error distribution from these measurements will be analyzed. This chapter is based on [28].

2.1 Introduction to the ^{7}Li Abundance Problem

The production of the light elements D, ^{3}He, ^{4}He, and ^{7}Li within the first 20 minutes after the Big Bang can be predicted from the standard Big Bang Nucleosynthesis (BBN) model. This is done by determining the cosmic baryon density of the Universe, Ω_b, which has recently been constrained by *WMAP* and *Planck* cosmic microwave background (CMB) data (see [29] and [30]). The prediction of D, ^{3}He and ^{4}He abundances are in good accordance with observations. However, the observed ^{7}Li abundance appears to be depleted by a factor of about three compared to predictions, and so has an obvious discrepancy.[1]

[1]For reviews on the matter, see [31], [32], [33], [34], [35], [1], and [36]

Old main-sequence and subgiant stars that are formed from the primordial clouds are believed to preserve their lithium abundance, and thus it is best to observe ^{7}Li in the atmosphere of these stars. It is not beneficial to sample very metal-poor stars as they may not represent a lithium-rich star. Because of the fragility of this isotope, stars with deep convections (for example, very hot stars) should also not be sampled. The convection in these stars will mix the atmosphere with deeper layers of the star thus destroying the ^{7}Li. Warm, metal-poor dwarf stars (like turn-off stars) then have good representations of this elemental abundance, as it is thought to be best preserved here (see [1]). However, observations show that the ^{7}Li abundance, A(Li), is measured lower than what is expected by the BBN model. This is illustrated in Figure 2.1 where the majority of measurements lie on the so-called "Spite Plateau." There is a factor of about three discrepancy between the Spite Plateau measurements and those predicted by baryon density from WMAP.

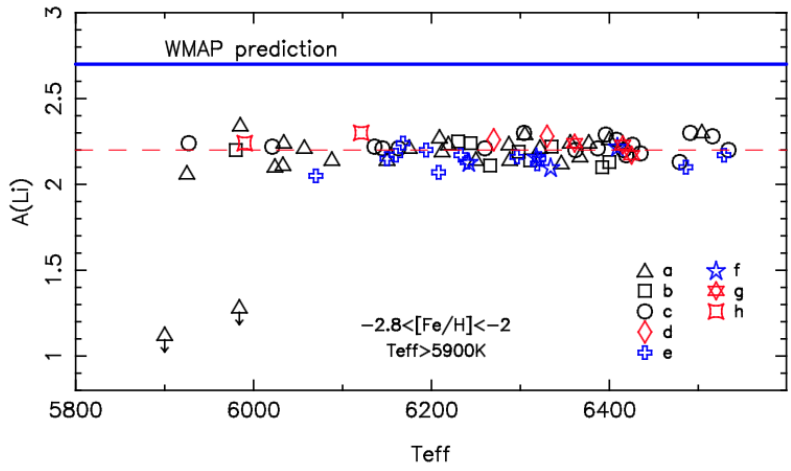

Figure 2.1: *Plot from [1] that shows the factor of three discrepancy between observed ^{7}Li abundance measurements and those predicted by the baryon density from WMAP. Note that the abundances are measured in dex which is a log based scale. For individual measurements, see reference therein.*

Some have argued for higher observed primordial A(Li) that is consistent with that expected from baryon density determined by CMB anisotropy data (See [37], [38], and [39]). It is of interest, however, to follow the popular belief that the standard BBN model

has a ^{7}Li problem. The attempt to quantify this discrepancy by use of non-Gaussian error distributions is done in this chapter.[2]

2.2 Data Selection of ^{7}Li Measurements

In this work, 66 A(Li) measurements are selected from [1]. Following [1], only stars within the metallicity range -2.8≤ [Fe/H] ≤-2.0 are considered in order to ensure that the abundances are representative of stars formed from primordial clouds.[3] A larger metallicity would represent a star that is too young to be considered, while a smaller metallicity star fails to lie on the "Spite Plateau" seen in Figure 2.1. As mentioned in Section 2.1, warm metal-poor stars with an effective temperature $T_{\rm eff} \geq 5900$ K should be considered such that the A(Li) in the atmosphere has not been depleted due to deep convection. With these constraints, [1] quote 77 A(Li) measurements. This work does not consider two of them as they are upper bounds. Of the remaining 75 measurements that give a mean and 1σ error of A(Li)$= 2.20 \pm 0.064$, nine do not quote error bars.[4] These 66 A(Li) measurements listed in Table 2.1[5] give a median and 1σ symmetrized error of A(Li)$= 2.21 \pm 0.065$.

[2]See [40], [41], [42], [34], [43], [44], [45], and [46] for discussions on possible mechanisms explaining this discrepancy.

[3]For an illustration, see Figure 2 of [1]. This figure includes stars with a metallicity of -5.0≤ $[Fe/H]$ ≤-2.0, and the scatter of stars below the Spite Plateau is obvious.

[4]These nine measurements do quote an error of $\sigma = 0.01$, but this only account for the signal to noise (S/N) ratio. As such, they are not included in this analysis.

[5]The errors given in this table from corresponding references are found by adding in quadrature errors from stellar parameters and from equivalent widths. However, [47] argue that the the stellar effective temperature error dominates all others and so the total error should be dominated and given by the effective temperature, and will therefore be constant. Given that the A(Li) error distribution is found to be non-Gaussian, possibly due to the result of unaccounted-for systematic error, this analysis is repeated for a constant error of $\sigma = 0.006$ in Appendix A.

Table 2.1: *66 Lithium Abundance Measurements*

Star Number/Name	A(Li)[a]	σ^{l}[b]	σ^{u}[b]	Reference
47480	2.17	0.061	0.061	
23344	2.13	0.026	0.026	
36513	2.15	0.094	0.078	
61361	2.25	0.063	0.027	
106468	2.24	0.025	0.024	
65206	2.07	0.057	0.048	
87467	2.25	0.067	0.057	
34630	2.12	0.052	0.049	
72461	2.22	0.066	0.059	
8572	2.24	0.027	0.026	
96115	2.22	0.028	0.021	
88827	2.31	0.052	0.048	[48]
68321	2.15	0.033	0.031	
48152	2.25	0.029	0.027	
12529	2.22	0.024	0.046	
61545	2.15	0.075	0.062	
59109	2.27	0.057	0.059	
59376	2.11	0.019	0.020	
36430	2.35	0.042	0.040	
87693	2.20	0.041	0.045	
111372	2.28	0.086	0.096	
102337	2.30	0.062	0.053	
115704	2.15	0.038	0.041	
LP0815-0043	2.20	0.035	0.035	
BD-13 3442	2.18	0.035	0.035	
BD+03 0740	2.17	0.035	0.035	
BD+09 2190	2.13	0.035	0.035	
BD+24 1676	2.21	0.035	0.035	
LP0635-0014	2.28	0.035	0.035	
CD-35 14849	2.29	0.035	0.035	
BD-10 0388	2.21	0.035	0.035	
BD-04 3208	2.30	0.035	0.035	
HD 338529	2.23	0.035	0.035	[38]
BD+02 3375	2.21	0.035	0.035	
HD 084937	2.26	0.035	0.035	
G011-044	2.30	0.035	0.035	
HD 24289	2.24	0.035	0.035	
BD+34 2476	2.23	0.035	0.035	
BD+42 3607	2.22	0.035	0.035	
BD+09 0352	2.21	0.035	0.035	
HD 19445	2.22	0.035	0.035	
HD 74000	2.20	0.035	0.035	
+26 3578	2.28	0.070	0.070	[49]
042-003	2.26	0.070	0.070	
BD+03° 740	2.13	0.074	0.074	
BD+09° 2190	2.10	0.084	0.084	
BD-13° 3442	2.15	0.057	0.057	
BD+26° 2621	2.17	0.070	0.070	
BD+20° 2030	2.07	0.068	0.068	
LP815-43	2.17	0.070	0.070	
BD+24° 1676	2.16	0.009	0.009	[50]
LP635-14	2.12	0.074	0.074	
CD-71° 1234	2.20	0.035	0.035	
BD+26° 3578	2.15	0.053	0.053	
CD-35° 14849	2.24	0.025	0.025	
HD84937	2.17	0.066	0.066	
HD74000	2.05	0.083	0.083	
CS29518-020	2.13	0.090	0.090	
CS30301-024	2.10	0.090	0.090	[47]
CS29499-060	2.16	0.090	0.090	
CS31061-032	2.22	0.090	0.090	
BS17572-100	2.17	0.090	0.090	
CS22950-173	2.23	0.090	0.090	[51]
CS29514-007	2.24	0.090	0.090	
G37-37	2.24	0.120	0.120	[52]
G130-65	2.30	0.120	0.120	

[a] Following the advice of M. Spite, for stars with both a main sequence and a sub-giant branch lithium abundance measurement, we list the average of the two values.

[b] σ^{l} and σ^{u} are the Lower 1σ and Upper 1σ errors respectively.

2.3 Error Distributions and Gaussian Tests of ^{7}Li Measurements

In order to test the Gaussianity of the remaining 66 A(Li) measurements, a central estimate must first be found. This is done by using both median and weighted mean statistics following Section 1.1. By Equation 1.1 the weighted mean estimate is given by

$$\mathrm{A(Li)}_{\mathrm{wm}} = \frac{\sum_{i=1}^{N} \mathrm{A(Li)}_i/\sigma_i^2}{\sum_{i=1}^{N} 1/\sigma_i^2}, \tag{2.1}$$

and the weighted error[6] by

$$\sigma_{\mathrm{wm}} = \left(\sum_{i=1}^{N} 1/\sigma_i^2 \right)^{-1/2} \tag{2.2}$$

from Equation 1.2. The goodness of fit is then given by

$$\chi_\nu^2 = \frac{1}{N-1} \sum_{i=1}^{N} \frac{(\mathrm{A(Li)}_i - \mathrm{A(Li)}_{\mathrm{wm}})^2}{\sigma_i^2} \tag{2.3}$$

from Equation 1.3. Weighted mean statistics gives a central estimate of $\mathrm{A(Li)}_{\mathrm{wm}} = 2.20$ with a weighted error of $\sigma_{\mathrm{wm}} = 4.43 \times 10^{-3}$. The goodness of fit analysis gives $\chi_\nu^2 = 2.41$ and $N_\sigma = 6.28$ (a fairly large number and a possible indication of non-Gaussianity).

The median statistics central estimate is found by the methods described in the same section. Using this method, a central estimate is found to be $\mathrm{A(Li)}_{\mathrm{med}} = 2.21$ with a 1σ range of $2.13 \leq \mathrm{A(Li)}_{\mathrm{med}} \leq 2.26$ and a 2σ range of $2.05 \leq \mathrm{A(Li)}_{\mathrm{med}} \leq 2.31$.[7]

These estimates are in good accordance with [1] who use a (non-weighted) mean to find an estimate of $\mathrm{A(Li)} = 2.20 \pm 0.064$ for the 75 original abundance measurements.

[6] For measurements with non-symmetric quoted errors, the average of the upper and lower errors are used for the weighted mean.

[7] Because median statistics does not make use of an individual measurement's associated error, a central estimate can be found for the 75 measurements (77 original measurements from [1] minus the two upper bound measurements). This yields an estimate of $\mathrm{A(Li)}_{\mathrm{med}} = 2.21$ with a 1σ and 2σ range of $2.13 \leq \mathrm{A(Li)}_{\mathrm{med}} \leq 2.26$ and $2.07 \leq \mathrm{A(Li)}_{\mathrm{med}} \leq 2.31$ respectively.

Following [25] an error distribution can now be constructed using the weighted mean and median central estimates. By Equation 1.10 and 1.11, where x_{CE} is either $A(Li)_{wm}$ or $A(Li)_{med}$, an N_σ for each value is found. As described in Section 1.4, N_σ is the number of standard deviations that a value deviates from the central estimate. Figure 2.2 shows the distribution of the signed and absolute N_σ using both central estimates.

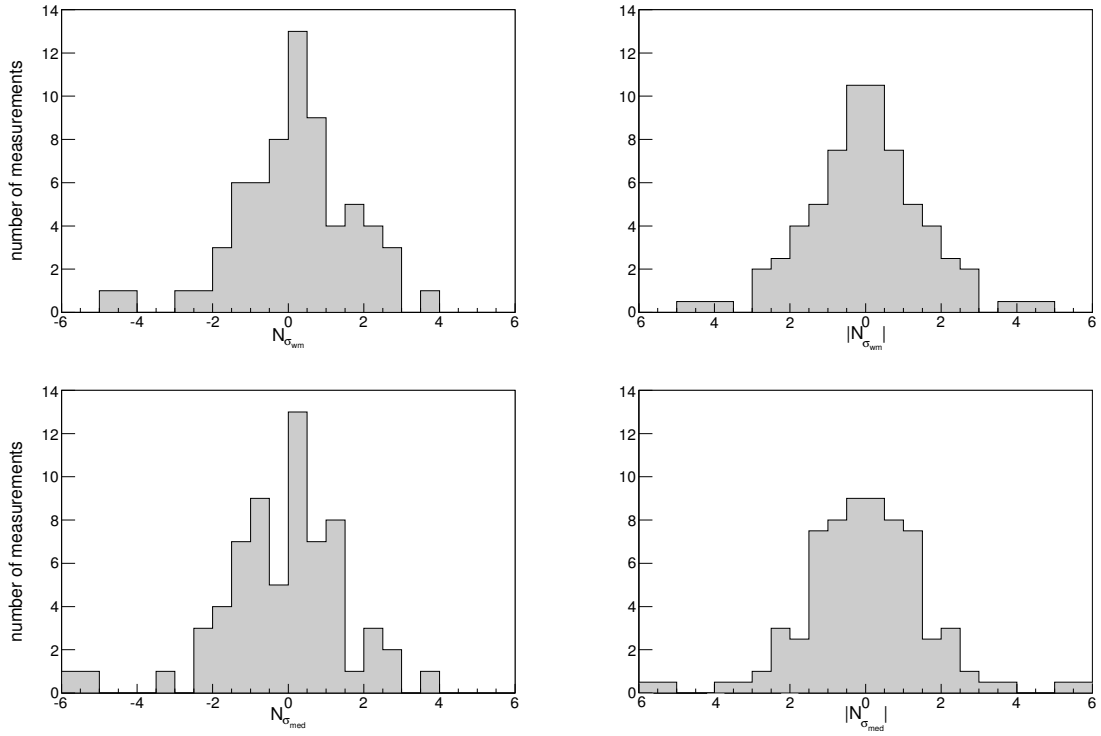

Figure 2.2: *Histogram of the error distribution of 66 A(Li) measurements in half standard deviation bins. The top (bottom) plot uses the weighted mean (median) central estimate for N_σ. The left and right plots are the signed and absolute, or symmetric, distributions respectively.*

Quantitatively, by using the weighted mean statistics, 68.3% of the signed error distribution falls within -1.88$\leq N_\sigma \leq$ 1.15 and 95.4% falls within -4.53$\leq N_\sigma \leq$ 2.03. The absolute magnitude of the error distribution has corresponding limits of $|N_\sigma| \leq 1.41$ and $|N_\sigma| \leq 3.0$ (see the second to last line of Table 2.3). Alternatively, the fraction of the data that falls within the $|N_\sigma| = 1$ and $|N_\sigma| = 2$ ranges are 54.5% and 81.8%, respectively. For the median statistics case, 68.3% of the signed error distribution falls within -1.75$\leq N_\sigma \leq$ 1.15 and

95.4% falls within -5.56$\leq N_\sigma \leq$ 2.25. The absolute magnitude of the error distribution have corresponding limits of $|N_\sigma| \leq 1.31$ and $|N_\sigma| \leq 3.10$ (see the last line of Table 2.3). The fraction of the data that falls within the $|N_\sigma| = 1$ and 2 ranges are 51.5% and 81.8%, respectively. For a Gaussian distribution, 68.3% of the signed error distribution falls within -1.00$\leq N_\sigma \leq$ 1.00 and 95.4% falls within -2.00$\leq N_\sigma \leq$ 2.00, and so the A(Li) measurement error distribution appears to be non-Gaussian.

It is now of interest to fit other well-known non-Gaussian distributions to the measurements. In this analysis, a parametric χ^2 test following Section 1.5 is used.[8] The 66 measurements are binned to 8 bins ($T = 8$) labeled by integer $j = 1, 2, ..., 8$ with varying bin widths to allow about 8 measurements per bin. Therefore, for any assumed distribution $P(|N_\sigma|)$, each bin should be expected to contain 8.25 measurements.

Using Equation 1.12 a goodness of fit can be found. Reduced χ^2, $\chi^2_\nu = \chi^2/\nu$, is also found. In this case, ν is 8 minus the number of fitting parameters and constraints. Without any other free parameters, $\nu = 7$. The symmetric $|N_\sigma|$ distribution is now fit to four well-know probability distribution functions: the Gaussian, described in Section 1.2, and the Lorentzian, Student's t, & double exponential described in Section 1.3. The error distribution will also be scaled by factor S, that is $|N_\sigma|/S$, to minimize χ^2. S will vary over 0.1-3.0 in steps of 0.1. When $S \neq 1$, the number of degrees of freedom reduces by one ($\nu = 6$). Although the possible non-Gaussianity of the A(Li) measurements has already been noted, the Gaussian probability distribution function will still be used to fit the distribution. Table 2.2 shows the reduced χ^2_ν and probabilities for the $S = 1$ and S corresponding to the minimized χ^2_ν cases for each of the four distributions.

Figure 2.3 shows the fitting of the distribution to the Gaussian probability distribution function (Equation 1.5) after normalization to unity. In allowing a scale factor, χ^2 is minimized by $S = 1.7$ ($S = 1.8$) for the weighted mean (median) case with a probability of $< 0.1\%$. Then 68.3% and 95.4% of the measurements fall within $|N_\sigma| = 1.7$ and $|N_\sigma| = 3.4$

[8] Moving forward, this analysis will make use of only the symmetric $|N_\sigma|$.

Table 2.2: *Goodness-of-Fit for Lithium Abundance Error Distribution*

	Weighted Mean				Median			
Function	Scale[a]	χ^{2b}_ν	ν[b]	Probability(%)[c]	Scale[a]	χ^{2b}_ν	ν[b]	Probability(%)[c]
Gaussian.....	1	65.8	7	< 0.1	1	101	7	< 0.1
Gaussian.....	1.7	10.9	6	< 0.1	1.8	11.5	6	< 0.1
Cauchy.....	1	6.70	7	< 0.1	1	7.31	7	< 0.1
Cauchy.....	1.6	5.54	6	< 0.1	1.6	6.00	6	< 0.1
$n = 8$ Student's t[d].....	1	25.3	6	< 0.1	1	30.4	6	< 0.1
$n = 8$ Student's t.....	2.6	2.04	5	6.9	2.8	2.16	5	5.5
Double Exponential.....	1	10.5	7	< 0.1	1	12.4	7	< 0.1
Double Exponential.....	1.4	8.76	6	< 0.1	1.5	9.94	6	< 0.1

[a] For a Gaussian distribution, $N_\sigma = 1$ corresponds to 1 standard deviation when the scale factor $S = 1$. For the other cases, the scale factor varies with the width of the distribution to allow χ^2 to be minimized.

[b] χ^2_ν is the χ^2 divided by the number of degrees of freedom ν.

[c] The probability that a random sample of data points drawn from the assumed distribution yields a value of χ^2_ν greater than or equal to the observed value for ν degrees of freedom. This probability assumes that the bins are uncorrelated, which is not necessarily true. Therefore, the probabilities should only be viewed as qualitative indicators of goodness of fit.

[d] We find that for the Student's t distribution, the $n = 2$ and $S = 1$ case gives a smaller reduced $\chi^2_\nu = 8.25$ (8.89) with a probability of < 0.1 (< 0.1) for the weighted mean (median) case. However, when allowing the scale factor S to vary, the $n = 8$ case has a lower reduced χ^2_ν than the $n = 2$ case.

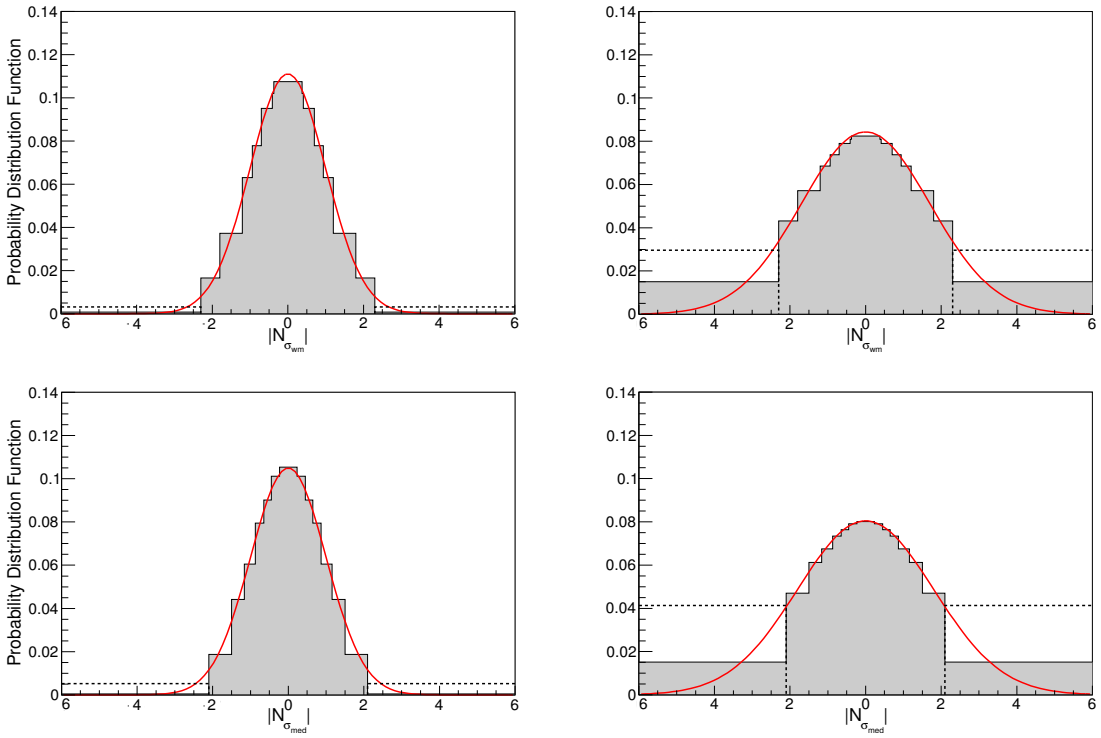

Figure 2.3: *Best fit Gaussian probability distribution function. The top plots show the fit to the* $|N_{\sigma_{\rm wm}}|$ *distribution with the left (right) showing a* $S = 1$ *(*$S = 1.7$*) scale factor. The bottom plots show the fit to the* $|N_{\sigma_{\rm med}}|$ *distribution with the left (right) showing a* $S = 1$ *(*$S = 1.8$*) scale factor. The dotted lines represent the expected probability of the last bins brought in from* $|N_\sigma| = \inf$ *to* $N_\sigma| = 6$ *with their heights adjusted to maintain the same probability.*

respectively for the weighted mean case, and $|N_\sigma| = 1.8$ and $|N_\sigma| = 3.6$ for the median case (see Table 2.3). Alternatively, for weighted mean statistics, 44% and 76% of the measurements fall within $|N_{\sigma_{\rm wm}}| \leq 1$ and $|N_{\sigma_{\rm wm}}| \leq 2$ respectively, while for median statistics, 42% and 73% fall within $|N_{\sigma_{\rm wm}}| \leq 1$ and $|N_{\sigma_{\rm wm}}| \leq 2$ (see Table 2.4). These values give evidence that the error distribution of the A(Li) measurements is non-Gaussian.[9]

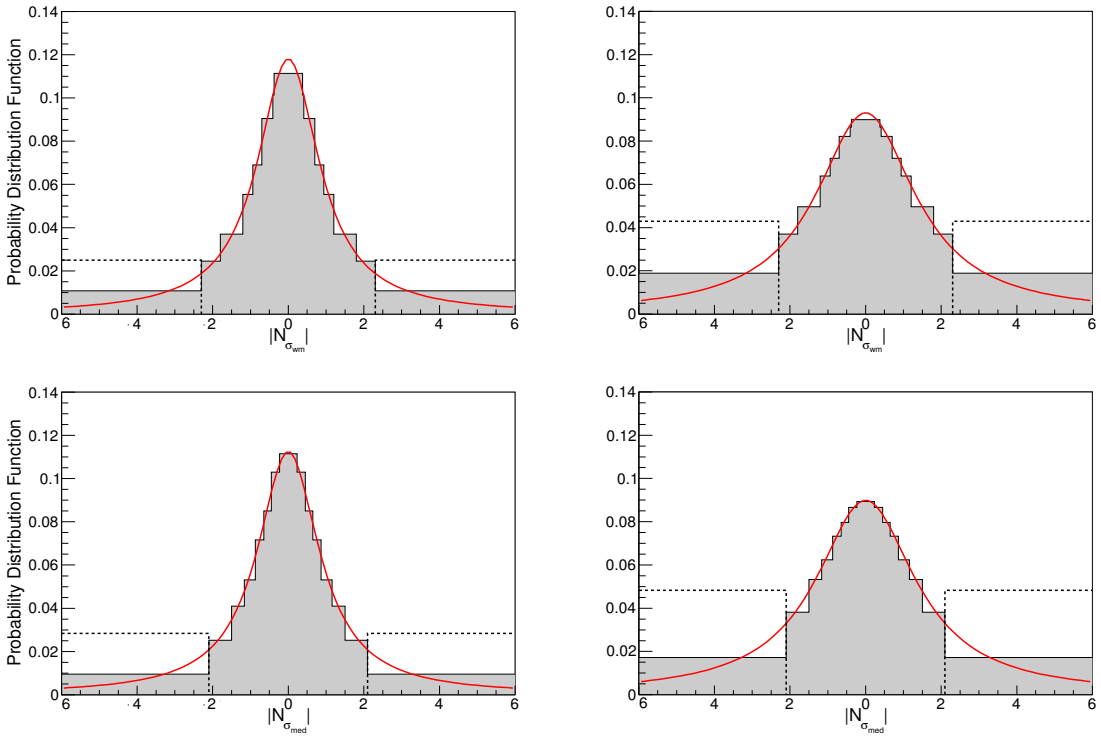

Figure 2.4: *Best fit Lorentzian probability distribution function. The top plots show the fit to the* $|N_{\sigma_{\rm wm}}|$ *distribution with the left (right) showing a* $S = 1$ *(*$S = 1.6$*) scale factor. The bottom plots show the fit to the* $|N_{\sigma_{\rm med}}|$ *distribution with the left (right) showing a* $S = 1$ *(*$S = 1.6$*) scale factor. The dotted lines represent the expected probability of the last bins brought in from* $|N_\sigma| = \inf$ *to* $N_\sigma| = 6$ *with their heights adjusted to maintain the same probability.*

It is then natural to fit to the first non-Gaussian probability distribution function: the Lorentzian given by Equation 1.6. Figure 2.4 shows the best fits, which favor an $S = 1.6$ scale factor for both the weighted mean and median cases. A scale factor of $S = 1$ has

[9]Although the error distributions of the lithium abundance measurements are non-Gaussian, this does not necessarily imply that the measurement errors themselves are non-Gaussian. Instead, it perhaps tells us something about the observers' ability to correctly estimate systematic and statistical uncertainties.

a probability of $< 0.1\%$. While the probability for $S = 1.6$ has the same probability, the χ^2_ν does decrease by a factor of two as compared to the Gaussian. There is an apparent increase in probability in the tails, as 68.3% and 95.4% fall within $|N_\sigma| \leq 2.9$ and $|N_\sigma| \leq 22$ respectively (see Table 2.3).

The observed error distribution has limits $|N_\sigma| \leq 1.4$ and $|N_\sigma| \leq 3.0$, and so a better fit may be one with wider tails than the Gaussian, but less so than the Lorentzian. A Student's t probability distribution function fits this description and is given by Equation 1.7.[10] The best fit, represented by an $S = 2.6$ and $n = 8$ ($S = 2.8$ and $n = 8$) for the weighted mean (median) case, for this function is seen in Figure 2.5. Here, n was allowed to vary between 2 and 30.[11] These best fits result in the highest probabilities of 6.9% and 5.5% for the weighted mean and median cases (Table 2.2). With the weighted mean (median) Student's t fit, only 29% (27%) of the data falls within $|N_\sigma| < 1$, and 68.3% of the data falls within $|N_\sigma| < 2.8$ ($|N_\sigma| < 3.0$) as expressed in Table 2.3 and Table 2.4.

Finally, the distribution is fit to a Double Exponential probability distribution function described by Equation 1.8. Figure 2.6 shows the best fit with scale factors $S = 1.4$ and $S = 1.5$ for the weighted mean and median cases. This scaling results in 68.3% of the measurements within $|N_\sigma| = 1.6$ ($|N_\sigma| = 1.7$) and 95.4% within $|N_\sigma| = 4.3$ ($|N_\sigma| = 4.6$) for the weighted mean (median) case (see Table 2.3). The probabilities for both central estimates are $< 0.1\%$ (Table 2.2).

2.4 Conclusions

Using 66 ^{7}Li abundance measurements from [1], an attempt has been made to try to quantify the discrepancy between expected and observed lithium. Confirming [32], the A(Li) error

[10] Note that this function reduces the number of degrees of freedom, ν, by one.

[11] When allowing n to vary, a pattern begins to form that results in a progressively better fit for every even value of n. For the smallest χ^2_ν for each value of n, S will rise (exceeding the upper bound of 3 on S). For $n = 10$ and $S = 3.1$ there is a reduced χ^2 probability of $\sim 29\%$, for $n = 12$ and $S = 3.8$ the probability is $\sim 61\%$, for $n = 14$ and $S = 4.7$ the probability is $\sim 86\%$. For $n = 20$, for $S > 1000$, χ^2_ν shows very gradual change, while still minimizing, resulting in a probability of $\sim 99.9\%$.

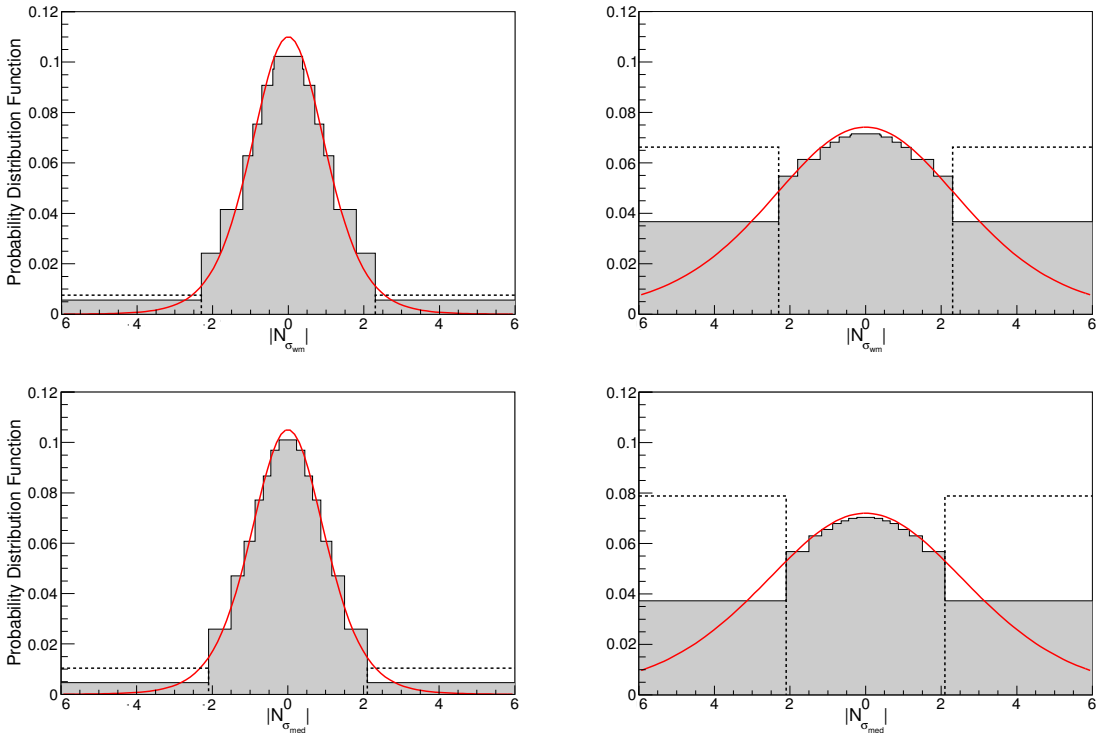

Figure 2.5: *Best fit Student's t probability distribution function. The top plots show the fit to the* $|N_{\sigma_{\mathrm{wm}}}|$ *distribution with the left (right) showing a* $S = 1$ *(*$S = 2.6$*) scale factor and* $n = 8$*. The bottom plots show the fit to the* $|N_{\sigma_{\mathrm{med}}}|$ *distribution with the left (right) showing a* $S = 1$ *(*$S = 2.8$*) scale factor and* $n = 8$*. The dotted lines represent the expected probability of the last bins brought in from* $|N_\sigma| = \inf$ *to* $N_\sigma| = 6$ *with their heights adjusted to maintain the same probability.*

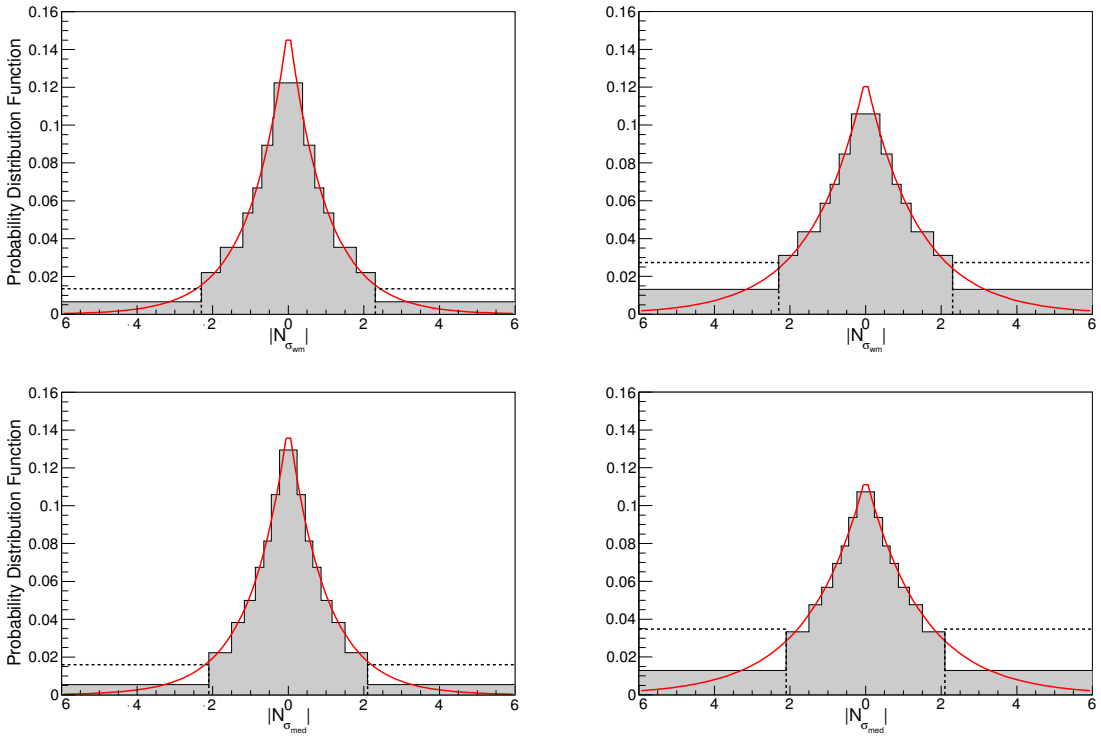

Figure 2.6: *Best fit double exponential probability distribution function. The top plots show the fit to the* $|N_{\sigma_{\rm wm}}|$ *distribution with the left (right) showing a* $S = 1$ *(*$S = 1.4$*) scale factor. The bottom plots show the fit to the* $|N_{\sigma_{\rm med}}|$ *distribution with the left (right) showing a* $S = 1$ *(*$S = 1.5$*) scale factor. The dotted lines represent the expected probability of the last bins brought in from* $|N_\sigma| = \inf$ *to* $N_\sigma| = 6$ *with their heights adjusted to maintain the same probability.*

Table 2.3: $|N_\sigma|$ *Limits*[a] *for Lithium Abundance Measurements*

Function	Scale[b]	68.3%[c]	95.4%[c]
Gaussian	1	1.0	2.0
Gaussian	1.7	1.7	3.4
Gaussian	1.8	1.8	3.6
Cauchy	1	1.8	14
Cauchy	1.6	2.9	22
Cauchy	1.6	2.9	22
$n = 8$ Student's t	1	1.1	2.4
$n = 8$ Student's t	2.6	2.8	6.1
$n = 8$ Student's t	2.8	3.0	6.6
Double Exponential	1	1.2	3.1
Double Exponential	1.4	1.6	4.3
Double Exponential	1.5	1.7	4.6
Observed Weighted Mean		1.4	3.0
Observed Median		1.3	3.1

[a] For each set of named distribution functions, the first line is for the standard distribution and the second and third lines are for the distributions that best fit the error distribution constructed using the weighted mean and median central estimate respectively.

[b] For a Gaussian distribution, $N_\sigma = 1$ corresponds to 1 standard deviation when the scale factor is $S = 1$. For the other functions, unless $S = 1$, the scale factor varies with the width of the distribution to allow χ^2 to be minimized.

[c] The $|N_\sigma|$ limits that contain 68.3% and 95.4% of the probability.

Table 2.4: *Expected Fractions*[a] *for Lithium Abundance Measurements*

Function	Scale[b]	$\lvert N_\sigma \rvert \leq 1$[c]	$\lvert N_\sigma \rvert \leq 2$[c]
Gaussian	1	0.68	0.95
Gaussian	1.7	0.44	0.76
Gaussian	1.8	0.42	0.73
Cauchy	1	0.50	0.71
Cauchy	1.6	0.36	0.57
Cauchy	1.6	0.36	0.57
$n = 8$ Student's t	1	0.65	0.92
$n = 8$ Student's t	2.6	0.29	0.54
$n = 8$ Student's t	2.8	0.27	0.50
Double Exponential	1	0.63	0.87
Double Exponential	1.4	0.51	0.76
Double Exponential	1.5	0.49	0.74
Observed Weighted Mean		0.55	0.82
Observed Median		0.52	0.82

[a] For each set of named distribution functions, the first line is for the standard distribution and the second and third lines are for the distributions that best fit the error distribution constructed using the weighted mean and median central estimate respectively.

[b] For a Gaussian distribution, $N_\sigma = 1$ corresponds to 1 standard deviation when the scale factor is $S = 1$. For the other functions, unless $S = 1$, the scale factor varies with the width of the distribution to allow χ^2 to be minimized.

[c] The fraction of the area that lies within $\lvert N_\sigma \rvert = 1$ and $\lvert N_\sigma \rvert = 2$.

distribution is non-Gaussian. This may be a result of the observers' estimates of systematic and statistical uncertainties.[12] It may also be the case that higher-quality data is required.

It is then of interest to explore the statistical significance of the discrepancy. First, Gaussianity is assumed, and the difference between the *PLANCK* expected value, A(Li)= 2.69 (See [36]), and the median value from this analysis, A(Li)= 2.21, is found. Then dividing by the quadrature sum of this analysis' symmetrized error ($\sigma = 0.065$) and that from [36], ($\sigma = 0.034$), a discrepancy of 6.5σ is found. Now accounting for the non-Gaussianity, $\sigma = 0.065$ is multiplied by 1.4 (Table 2.3, second to last line)[13] in the quadrature sum. This reduces the discrepancy to 4.9σ.

In an attempt the characterize the A(Li) error distribution that has larger probability in the tails than a Gaussian distribution, it is fit to four well-known probability distribution functions. Allowing a scale factor to vary from $0.1 \leq S \leq 3.0$, the error distribution is best fit by an $n = 8$ Student's t distribution. However, this is unlikely to be of much physical significance.

While it would be beneficial to have more higher-quality measurements that would result in a Gaussian error distribution to be able to draw definite conclusions, it can be concluded that the non-Gaussianity of the current measurements cannot fully resolve the Li problem. However, the discrepancy is slightly reduced.

[12] See Appendix A.
[13] This is the observed weighted mean $|N_\sigma|$ limit.

Chapter 3

Non-Gaussian Error Distribution of LMC/SMC Distance Moduli Measurements

The nearby Large Magellanic Cloud galaxy gives rise to a well studied and documented number of distance moduli measurements. It is then of interest to examine these measurements, as the distance to this galaxy plays an important role in determining cosmological distances. Gaussian tests of the error distributions constructed from these measurements are used to possibly support publication bias and/or correlations between measurements as suggested by [2]. This chapter is based on [53].

3.1 Introduction to LMC Distance Moduli Measurements

The Large Magellanic Cloud (LMC) is a nearby galaxy within the Local Group with a plethora of stellar tracers. Because of the closeness and the abundance of tracers, it is

well studied and a large number of distance measurements to the LMC are available. The distance to this galaxy provides an important low rung in the cosmological distance ladder, and as such is important to analyze the available measurements. [2] has compiled (following [54]) 237 LMC distance moduli measurements published within the years 1990-2014. They used the compilation to examine the effects of publication bias, which they concluded to not be strong. However, correlations between measurements did have effects (especially in some individual tracer subsamples).

In this chapter, Gaussian tests of constructed error distributions are used to complement the analysis of [2]. This is done to the full 232 distance moduli measurement set[1] and two individual tracer subsamples (Cepheids and RR Lyrae).

3.2 Error Distribution and Gaussian Tests of Full LMC Distance Moduli Dataset

To analyze the full LMC distance moduli measurement dataset, an error distribution is constructed following [25] and [28]. This is a histogram of the number of standard deviations that a measurement deviates from a central estimate, N_σ (see Equation 1.9). Here,

$$N_{\sigma_i} = \frac{D_i - D_{\mathrm{CE}}}{(\sigma_i^2 + \sigma_{\mathrm{CE}}^2)^{1/2}} \tag{3.1}$$

where D_i and D_{CE} are the individual distance moduli measurement and central distance moduli measurement respectively. This is similar to the z score analysis of [2], however, they use two published values[2] assumed to well represent the measurements[3], whereas this analysis uses weighted mean and median statistics to find a central estimate.

The central estimates are found by the techniques described in Section 1.1. Here, the

[1] This analysis does not make use of five of the measurements from [2], as they do not have error bars.
[2] [55] and [56]
[3] Thus their analysis assumes Gaussianity.

weighted mean is

$$D_{\rm wm} = \frac{\sum_{i=1}^{N} D_i/\sigma_i^2}{\sum_{i=1}^{N} 1/\sigma_i^2}. \tag{3.2}$$

This analysis uses the quadrature sum of quoted statistical and systematic (if quoted) errors for σ_i. Many of the measurements do not have an associated systematic error, and if it is quoted it is small, thus it does not contribute much to the overall error.[4] The goodness of fit, χ^2_ν, is then

$$\chi^2_\nu = \frac{1}{N-1} \sum_{i=1}^{N} \frac{(D_i - D_{\rm wm})^2}{\sigma_i^2}. \tag{3.3}$$

The median central estimate is found as described in Section 1.1.

The distance moduli central estimate, when using weighted mean statistics, is $(m - M)_0 = 18.49 \pm 3.11 \times 10^{-3}$ mag. The goodness of fit yields $\chi^2_\nu = 3.00$, and the number of standard deviations that χ_ν deviates from unity is $N = 15.7$[5]. When using median statistics, the central estimate is $(m - M)_0 = 18.49$ mag with a 1σ range of 18.32 mag$\leq (m-M)_0 \leq$18.59 mag. [2] quote $(m-M)_0 = 18.49 \pm 0.09$ mag[6], and so the central estimates found in this analysis are in good accord.

An error distribution is now constructed using the two central estimates, seen in Figure 3.1. Both the signed N_σ and absolute, symmetrized ($|N_\sigma|$) are plotted. A more detailed distribution of $|N_\sigma| = 0.1$ bin size is shown in Figure 3.2

Qualitatively, one can see the extended tails present in the weighted mean error distribution. That is, there appears to be more probability in the tails as compared to a Gaussian distribution. Quantitatively, for a set of 232 values, a Gaussian distribution should yield 11 values within $|N_\sigma| \leq 2$, one within $|N_\sigma| \leq 3$, and none within $|N_\sigma| \leq 4$. The distribution from this analysis finds 42 values within $|N_\sigma| \leq 2$, 23 within $|N_\sigma| \leq 3$, and nine within $|N_\sigma| \leq 4$ (see Table 3.1). It can also be noted that 68.3% of the observed

[4] Of the 232 measurements under consideration, only 49 quote a non-zero systematic error. This is further discussed in the conclusion of this chapter (Section 3.6).

[5] A large number that may hint at non-Gaussianity.

[6] [2] use 233 distance moduli measurements published in years 1990 to 2013. We have used the updated 2014 measurements in addition to those previously published.

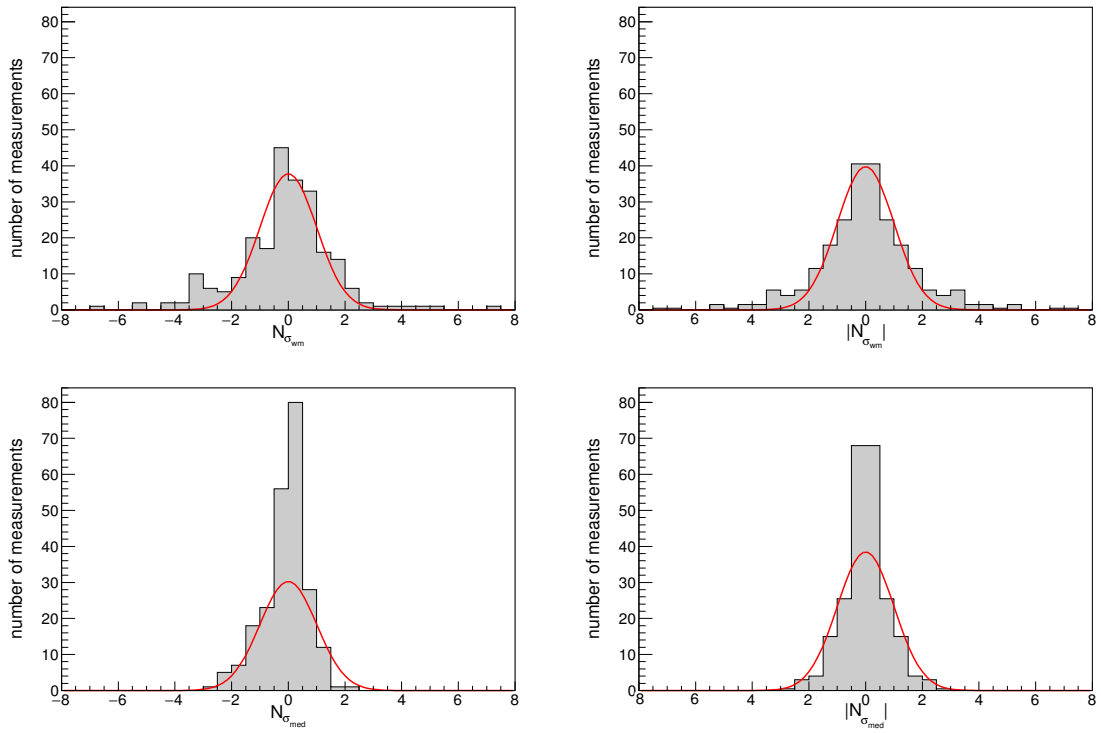

Figure 3.1: *Histogram of the error distribution of 232 LMC measurements in half standard deviation bins. The top (bottom) plots use the weighted mean (median) central estimate for N_σ. The left and right plots are the signed and absolute, or symmetric, distributions respectively. The smooth curve in each panel is the best-fit Gaussian.*

weighted mean N_σ error distribution falls within $-1.37 \leq N_\sigma \leq 1.26$, while 95.4% lies within $-3.37 \leq N_\sigma \leq 4.57$. The observed weighted mean $|N_\sigma|$ error distribution has limits of $|N_\sigma| \leq 1.33$ and $|N_\sigma| \leq 3.63$ respectively, and 56.5% and 81.9% of the values fall within $|N_\sigma| \leq 1$ and $|N_\sigma| \leq 2$ respectively. This distribution indicates that the weighted mean case is non-Gaussian, and so this technique is not appropriate for analyzing the LMC distance moduli measurements.

In the case of the median central estimate, the distribution is narrower than expected for a Gaussian. Note that the larger $\sigma_{\rm med}$ results in this.[7] There are seven values within $|N_\sigma| \leq 2$ and none within $|N_\sigma| \leq 3$. 68.3% of the data falls within $-0.86 \leq N_\sigma \leq 0.63$, while 95.4% lies within $-1.97 \leq N_\sigma \leq 1.27$. The $|N_\sigma|$ error distribution has limits of

[7]See Equation 3.1.

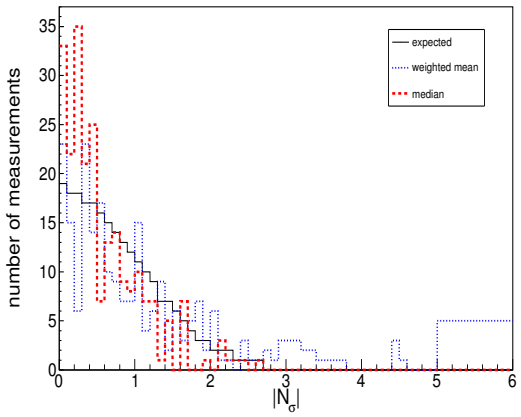

Figure 3.2: *Histogram of the error distribution of 232 LMC measurements in* $|N_\sigma| = 0.1$ *bins (with the exception of the last, truncated, bin with* $5 \leq |N_\sigma| \leq 6$ *that contains the number of measurements to* $|N_\sigma| = 8$*). The solid black line represents the expected Gaussian probabilities for a set of 232 measurements. The dotted blue (dashed red) line is the number of* $|N_\sigma|$ *values in each bin for the weighted mean (median) case.*

$|N_\sigma| \leq 0.72$ and $|N_\sigma| \leq 1.66$ respectively, and 80.6% and 97.0% of the values fall within $|N_\sigma| \leq 1$ and $|N_\sigma| \leq 2$ respectively. The median technique is more appropriate because of the apparent non-Gaussianity of the distributions. The narrowness of the median distribution is consistent with the presences of correlations between measurements, as suggested by [2]. The correlations would suggest that the measurements are not statistically independent, and the errors associated with the median will need to be slightly adjusted to account for this.

Because of the apparent non-Gaussianity of the error distribution, it is of interest to fit them to well-known probability distribution functions. This analysis will use a non-parametric test, the KS test, which is described in the last paragraph of Section 1.5. This test finds the compatibility of the distribution of measurements to a reference distribution, and will be done with both binned and un-binned measurements for this analysis.

To set conventions, even though the error distribution is non-Gaussian, it will be fit to a Gaussian probability distribution function (see Equation 1.5) where 68% of the values fall

Table 3.1: *Expected Gaussian and Observed Numbers of $|N_\sigma|$ for LMC Distance Moduli Measurements*

Tracer	Values[a]	$\lvert N_\sigma \rvert$	Expected[b]	Observed (WM)[c]	Observed (Med)[c]
All Types	232	≥ 0.5	143	151	96
		≥ 1	74	101	45
		≥ 1.5	31	65	15
		≥ 2	11	42	7
		≥ 2.5	3	31	1
		≥ 3	1	23	0
		≥ 4	0	9	0
Cepheids	81	≥ 0.5	50	48	34
		≥ 1	26	35	17
		≥ 1.5	11	20	4
		≥ 2	4	10	2
		≥ 2.5	1	7	1
		≥ 3	0	6	0
RR Lyrae	63	≥ 0.5	39	31	20
		≥ 1	20	20	11
		≥ 1.5	8	12	4
		≥ 2	3	7	1
		≥ 2.5	0	5	0
		≥ 3	0	3	0

[a] The number of distance moduli measurements used in this analysis.

[b] The number of values expected to fall outside of the corresponding $|N_\sigma|$ for a Gaussian distribution of total number listed in Col (2).s

[c] The observed number of values outside of the corresponding $|N_\sigma|$.

within $|N_\sigma| \leq 1$.[8] The compatibility given from this test yields a probability of $< 0.1\%$ for the Gaussian function (Table 3.2).

Next, three non-Gaussian probability distribution functions are used to fit the distribution. The Lorentzian distribution (see Equation 1.6), with 68% of the values falling within $|N_\sigma| \leq 1.8$, also gives probabilities of $< 0.1\%$ for both the binned and unbinned KS test. Fitting to the Student's t function (Equation 1.7) gives probabilities of $< 0.1\%$. Finally, the distribution is fit to a double exponential distribution (see Equation 1.8) where 68.3% of the values fall within $|N_\sigma| \leq 1.2$. Again, the probabilities are $< 0.1\%$.

Table 3.2: *K-S Test Probabilities for LMC Distance Moduli Measurements*

Function[a]	Data Set	Un-binned Probability(%)[b]	Binned Probability(%)[b]
Gaussian	Whole (232)	< 0.1	< 0.1
	Truncated (223)	< 0.1	< 0.1
	Cepheids (81)	1.5	< 0.1
	Truncated Cepheids (75)	2.8	0.10
	RR Lyrae (63)	1.5	< 0.1
	Truncated RR Lyrae (58)	0.8	< 0.1
Cauchy	Whole (232)	< 0.1	< 0.1
	Truncated (223)	< 0.1	< 0.1
	Cepheids (81)	1.0	< 0.1
	Truncated Cepheids (75)	2.9	< 0.1
	RR Lyrae (63)	1.6	< 0.1
	Truncated RR Lyrae (58)	0.7	< 0.1
Double Exponential	Whole (232)	< 0.1	< 0.1
	Truncated (223)	< 0.1	< 0.1
	Cepheids (81)	1.5	< 0.1
	Truncated Cepheids (75)	3.7	< 0.1
	RR Lyrae (63)	1.3	< 0.1
	Truncated RR Lyrae (58)	0.6	< 0.1
$n = 39$ Student's t	Whole (232)	< 0.1	< 0.1
$n = 13$ Student's t	Truncated (223)	< 0.1	< 0.1
$n = 13$ Student's t	Cepheids (81)	1.1	< 0.1
$n = 60$ Student's t	Truncated Cepheids (75)	3.1	< 0.1
$n = 87$ Student's t	RR Lyrae (63)	1.9	< 0.1
$n = 93$ Student's t	Truncated RR Lyrae (58)	0.9	< 0.1

[a] For the Student's t case, the n corresponding with the best probability is displayed.
[b] The probability that the data set is compatible with the assumed distribution.

From Figures 3.1 and 3.2 and Tables 3.1 and 3.2, it is clear that the weighted mean case

[8] The symmetric error distribution will be used moving forward.

has a distribution closer to a Gaussian near the peak, but also has an extended tail. This suggests the existence of unaccounted-for systematic errors, as the weighted mean makes use of an individual measurement's quoted error. For the median case, the peak is greater than a Gaussian and falls off more rapidly with increasing $|N_\sigma|$. This may point to correlations between measurements or possible publication bias.

It is then of interest to truncate the error distributions by removing all values with $|N_\sigma| \geq 4$.[9] Doing so gives 223 measurements with an unchanged, weighted mean central estimate of $(m-M)_0 = 18.49 \pm 3.38 \times 10^{-3}$. The goodness of fit gives $\chi^2_\nu = 1.90$ and $N = 8.01$. [10] Figure 3.3 shows the truncated weighted mean error distribution. Quantitatively, 68.3% of the values fall within $-1.55 \leq N_\sigma \leq 1.05$ and 95.4% fall within $-3.66 \leq N_\sigma \leq 2.06$. For the absolute case, $|N_\sigma| \leq 1.23$ and $|N_\sigma| \leq 3.03$ for 68.3% and 95.4% of the values ,respectively. In terms of percentages, 61.0% and 85.2% of the measurements fall within $|N_\sigma| \leq 1$ and $|N_\sigma| \leq 2$ respectively.[11]

Next, the truncated distribution is fit to the four probability distribution functions. All four distributions still yield a probability of $< 0.1\%$. There is still indication of non-Gaussianity because of the larger than expected $|N_\sigma| > 2$ and 3 tail.

3.3 Error Distributions and Gaussian Tests of 81 Cepheid Tracer Type Measurements

[2] note the possible correlations between measurements, especially within individual tracer types. It is then of interest to also investigate the error distributions of these measurements.

[9] For a Gaussian distribution with 232 measurements, there should be zero with $|N_\sigma| \geq 4$ (see Table 3.1.

[10] The truncated analysis was repeated for the median case (by removing nine values), but probabilities did not increase. This exemplifies the robustness of median statistics.

[11] It should be noted that when truncated, the normal standard deviation becomes $\sigma = 0.125$ while the symmetrized error for the median case is $\sigma = 0.126$. It would appear that after eliminating $|N_\sigma| > 4$, the median and weighted mean cases converge. However, we do utilize a weighted mean rather than the standard mean, as the errors for the measurements are not the same, and the weighted mean and median statistics error still do not converge even in the truncated case.

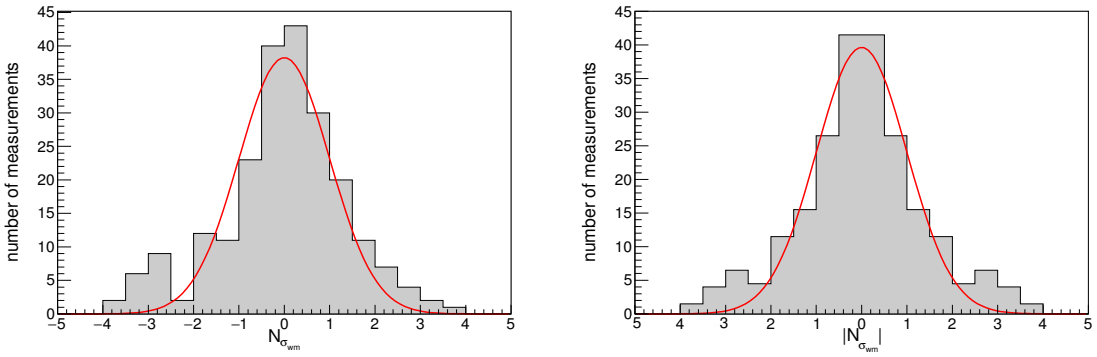

Figure 3.3: *Histogram of the error distribution of 223 LMC measurements in half standard deviation bins for truncated weighted mean distribution ($|N_\sigma| \geq 4$). The left and right plots are the signed and absolute, or symmetric, distributions respectively. The smooth curve in each panel is the best-fit Gaussian.*

First, 81 Cepheid distance moduli values from [2] are used. Weighted mean statistics gives a central estimate of $(m - M)_0 = 18.52 \pm 6.52 \times 10^{-3}$ mag.[12] For signed N_σ, 68.3% of the values fall within $-1.04 \leq N_\sigma \leq 1.73$ and 95.4% fall within $-1.78 \leq N_\sigma \leq 5.68$. For absolute N_σ, 68.3% and 95.4% of the values fall within corresponding limits $|N_\sigma| \leq 1.31$ and $|N_\sigma| \leq 4.13$. 56.8% of the values fall within $|N_\sigma| \leq 1$ and 87.7% fall within $|N_\sigma| \leq 2$.

The median case central estimate is $(m-M)_0 = 18.50$ mag with a 1σ range of 18.37 mag $\leq (m-M)_0 \leq 18.60$ mag. For signed N_σ, 68.3% of the values fall within $-0.67 \leq N_\sigma \leq 0.73$ and 95.4% fall within $-1.28 \leq N_\sigma \leq 1.76$. For absolute N_σ, 68.3% and 95.4% of the values fall within corresponding limits $|N_\sigma| \leq 0.71$ and $|N_\sigma| \leq 1.63$. 79.0% of the values fall within $|N_\sigma| \leq 1$ and 97.5% fall within $|N_\sigma| \leq 2$. This distribution is tighter as compared to that of 232 measurements.

Figure 3.4 shows the error distributions for the signed and absolute weighted mean and median cases. A more detailed plot with $|N_\sigma|$ in bins of 0.1 is shown in Figure 3.5. As with the full dataset, one can note the widened (narrowed) distribution for the weighted mean (median) case. The distribution of Cepheid tracer type measurements are also fit to the four well-known distributions. It is best fit equally by the Gaussian and double exponential

[12]The goodness of fit gives a $\chi^2 = 2.66$ and $N = 7.96$ which is the number of standard deviations that χ deviates from unity.

distributions with a corresponding probability of $< 1.5\%$ (Table 3.2).

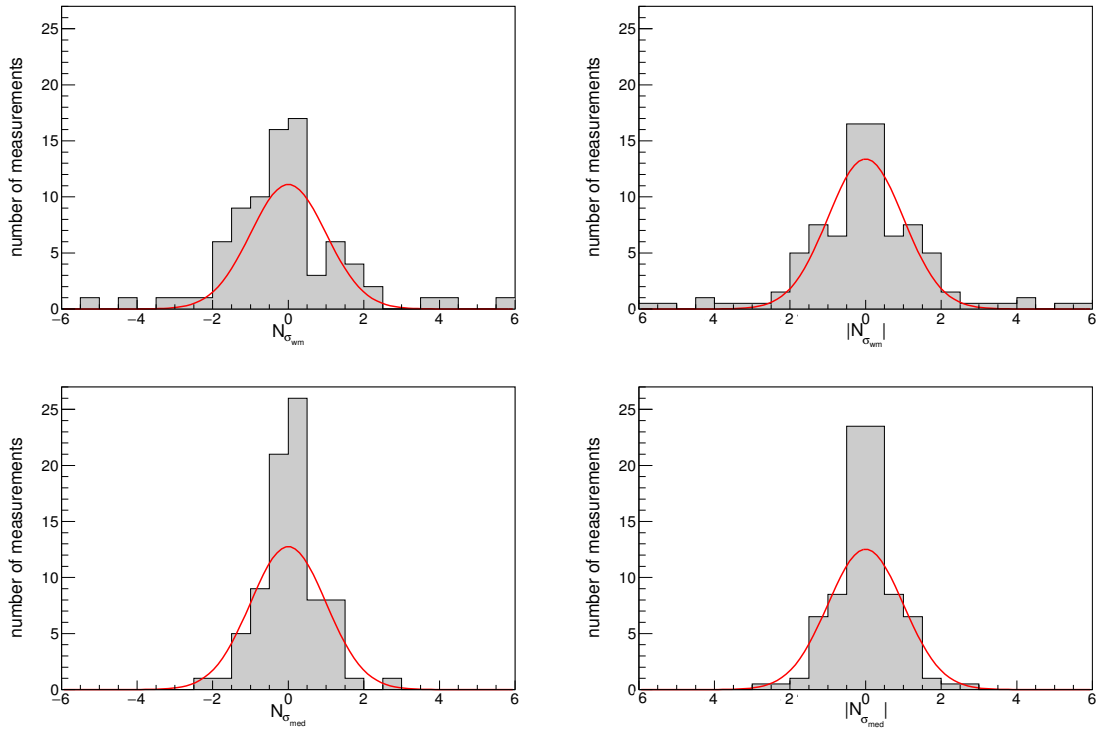

Figure 3.4: *Histogram of the error distribution of 81 LMC Cepheid tracer type measurements in half standard deviation bins. The top (bottom) plots use the weighted mean (median) central estimate for N_σ. The left and right plots are the signed and absolute, or symmetric, distributions respectively. The smooth curve in each panel is the best-fit Gaussian.*

The Cepheid sub-sample is also truncated by removing all values with $|N_\sigma| > 3$, as there should be none for a Gaussian distribution set of 81 measurements (see Table 3.1). This left 75 measurements. The median case remained unaffected (due to the robustness of median statistics), but the weighted mean case slightly tightened with a new central estimate of $(m - M)_0 = 18.51 \pm 7.27 \times 10^{-3}$ mag. For signed N_σ, 68.3% of the values fall within $-0.931 \leq N_\sigma \leq 1.48$ and 95.4% fall within $-2.43 \leq N_\sigma \leq 2.38$. For absolute N_σ, 68.3% and 95.4% of the values fall within $|N_\sigma| \leq 1.11$ and $|N_\sigma| \leq 2.23$, respectively. 65.3% of the values fall within $|N_\sigma| \leq 1$ and 94.7% fall within $|N_\sigma| \leq 2$. The un-binned KS test for the truncated Cepheid set gave a slight increase in probability of 3.7% for the double

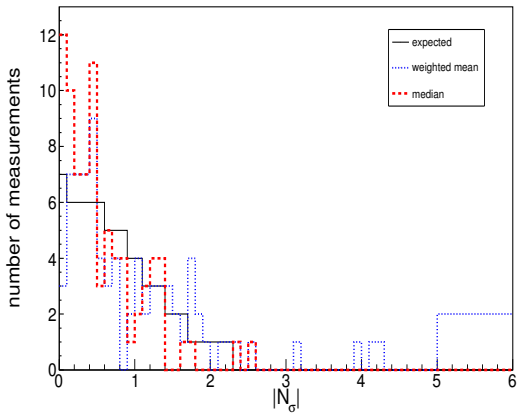

Figure 3.5: *Histogram of the error distribution of 81 LMC Cepheid tracer type measurements in $|N_\sigma| = 0.1$ bins (with the exception of the last, truncated, bin with $5 \leq |N_\sigma| \leq 6$). The solid black line represents the expected Gaussian probabilities for a set of 81 measurements. The dotted blue (dashed red) line is the number of $|N_\sigma|$ values in each bin for the weighted mean (median) case.*

exponential case (Table 3.2).

3.4 Error Distributions and Gaussian Tests of 63 RR Lyrae Tracer Type Measurements

When using 63 RR Lyrae distance moduli measurements[13] from [2], weighted mean statistics gave a central estimate of $(m - M)_0 = 18.48 \pm 1.03 \times 10^{-2}$ mag. For signed N_σ, 68.3% of the values fall within $-0.83 \leq N_\sigma \leq 1.15$ and 95.4% fall within $-1.75 \leq N_\sigma \leq 3.11$. For absolute N_σ, 68.3% and 95.4% of the values fall within $|N_\sigma| \leq 1.00$ and $|N_\sigma| \leq 3.11$, respectively. 68.3% of the values fall within $|N_\sigma| \leq 1$ and 88.9% fall within $|N_\sigma| \leq 2$.

For the median case we find a central estimate of $(m - M)_0 = 18.47$ mag with a 1σ range of 18.29 mag $\leq (m-M)_0 \leq$ 18.55 mag. For signed N_σ, 68.3% of the values fall within $-0.65 \leq N_\sigma \leq 0.48$ and 95.4% fall within $-1.50 \leq N_\sigma \leq 1.03$. For absolute N_σ, 68.3% and 95.4% of the values fall within $|N_\sigma| \leq 0.50$ and $|N_\sigma| \leq 1.56$, respectively. 82.5% of the

[13]Three RR Lyrae values from [2] quote a zero error and were not used in this analysis.

values fall within $|N_\sigma| \leq 1$ and 98.4% fall within $|N_\sigma| \leq 2$.

There error distributions for this sub-sample can be seen in Figure 3.6, with a more detailed plot shown in Figure 3.7. It is difficult to observe non-Gaussianity visually from these plots. The RR Lyrae measurements are then fit to the four distributions, and the largest probability of 1.9% comes from an $n = 87$ Student's t distribution (Table 3.2). This is only slightly greater than 1.5% given by the Gaussian fit.

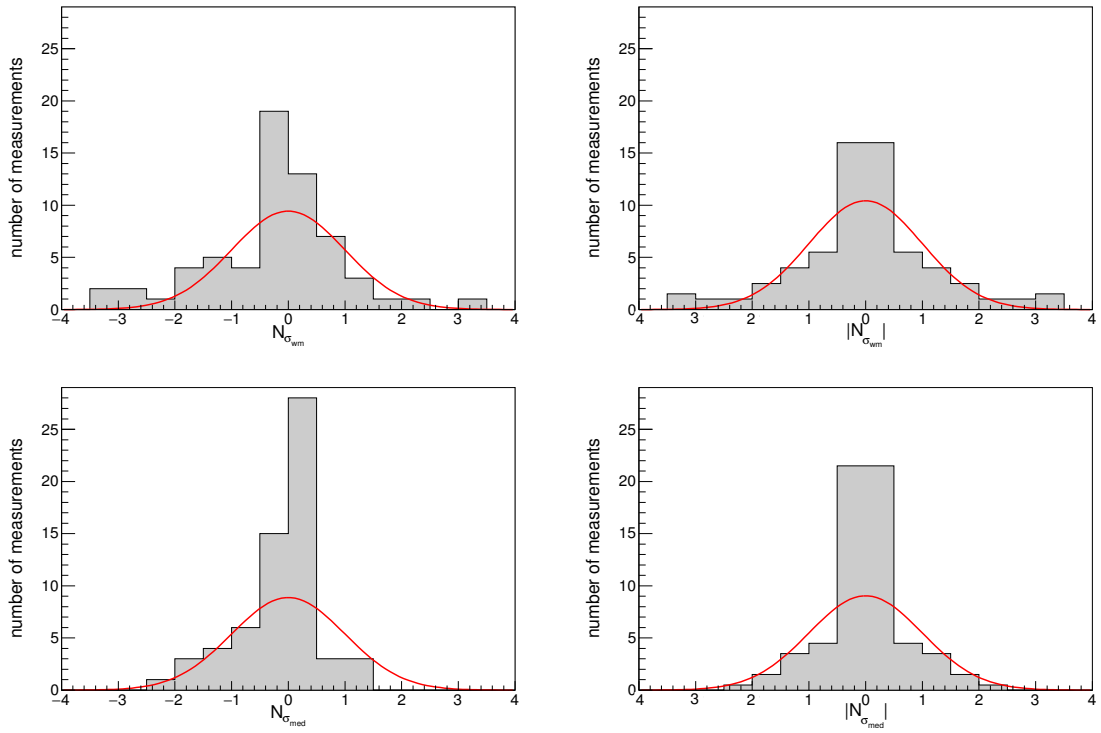

Figure 3.6: *Histogram of the error distribution of 63 LMC RR Lyrae tracer type measurements in half standard deviation bins. The top (bottom) plots use the weighted mean (median) central estimate for N_σ. The left and right plots are the signed and absolute, or symmetric, distributions respectively. The smooth curve in each panel is the best-fit Gaussian.*

This sub-sample is also truncated by removing all values $|N_\sigma| > 2.5$, as there should be none above this for a normally distributed set of 63 measurements (Table 3.1). The weighted mean error distribution is tightened by this truncation[14]. A central estimate is

[14]The median error distribution did not significantly change.

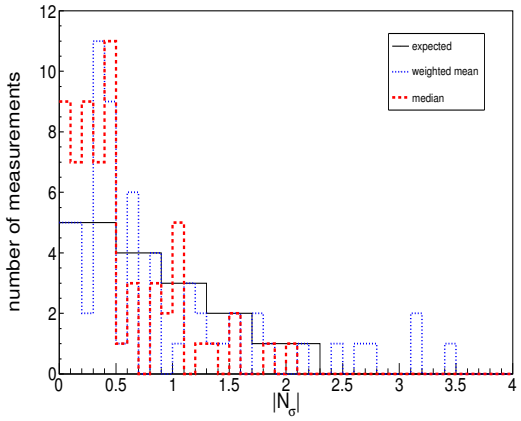

Figure 3.7: *Histogram of the error distribution of 63 LMC RR Lyrae tracer type measurements in $|N_\sigma| = 0.1$ bins). The solid black line represents the expected Gaussian probabilities for a set of 63 measurements. The dotted blue (dashed red) line is the number of $|N_\sigma|$ values in each bin for the weighted mean (median) case.*

found to be $(m - M)_0 = 18.49 \pm 1.10 \times 10^{-2}$ mag. For signed N_σ, 68.3% of the values fall within $-0.68 \leq N_\sigma \leq 0.79$ and 95.4% fall within $-2.49 \leq N_\sigma \leq 1.81$. For absolute N_σ, 68.3% and 95.4% of the values fall within $|N_\sigma| \leq 0.75$ and $|N_\sigma| \leq 1.87$ respectively, while 75.9% of the values fall within $|N_\sigma| \leq 1$ and 98.3% fall within $|N_\sigma| \leq 2$. This sub-sample is fit to the four distributions and all fits are decreased.[15]

3.5 Error Distributions and Gaussian Tests of SMC Distance Moduli Measurements

This analysis is repeated for 247 Small Magellanic Cloud (SMC) distance moduli measurements compiled by [57].[16] Weighted mean statistics gives a central estimate of $(m - M)_0 = 18.93 \pm 2.38 \times 10^{-2}$ mag. For signed N_σ, 68.3% and 95.4% of the measurements fall within $-2.01 \leq N_\sigma \leq 1.91$ and $-6.59 \leq N_\sigma \leq 4.76$, respectively. For the unsigned N_σ 68.3%

[15] Possibly due to the the small amount of measurements (58).

[16] [57] compiled a list of 304 measurements, but only those with non-zero quoted error were used in this analysis.

and 95.4% of the measurements have corresponding limits $|N_\sigma| \leq 1.91$ and $|N_\sigma| \leq 5.26$. Conversely, 45.8% of the measurements fall within $|N_\sigma| \leq 1$ and 70.5% fall within $|N_\sigma| \leq 2$. The extended tails in this distribution is non-Gaussian and may suggest unaccounted-for systematic errors.

For the median case, a central estimate of $(m - M)_0 = 18.94$ mag with a 1σ range of 18.81 mag $\leq (m - M)_0 \leq$ 19.08 mag is found. For signed N_σ, 68.3% and 95.4% of the measurements fall within $-0.80 \leq N_\sigma \leq 0.78$ and $-1.60 \leq N_\sigma \leq 2.91$ respectively. For the unsigned N_σ 68.3% and 95.4% of the measurements have corresponding limits $|N_\sigma| \leq 0.79$ and $|N_\sigma| \leq 1.68$. Conversely, 78.5% of the measurements fall within $|N_\sigma| \leq 1$ and 96.8% fall within $|N_\sigma| \leq 2$. This distribution is narrower than expected for a Gaussian and indicates possible correlations between measurements. [57] also suggest this, especially within sub-samples of individual tracer types.

In examining the Cepheid tracer type sub-sample, with 101 measurements, a central estimate of $(m-M)_0 = 18.98 \pm 4.17 \times 10^{-3}$ mag is found for the weighted mean case. 68.3% and 95.4% of the measurements are within $-1.55 \leq N_\sigma \leq 0.98$ and $-6.36 \leq N_\sigma \leq 1.76$ for signed N_σ. For the absolute case, $|N_\sigma| \leq 1.26$ and $|N_\sigma| \leq 4.02$ for 68.3% and 95.4% of the measurements, with 56.5% and 86.1% of the measurements falling within $N_\sigma \leq 1$ and $N_\sigma \leq 2$ respectively. Median statistics gives a central estimate of $(m - M)_0 = 18.98$ mag with a 1σ range of 18.83 mag $\leq (m-M)_0 \leq$ 19.13 mag. The distribution shows that 68.3% and 95.4% of the measurements are within $-0.83 \leq N_\sigma \leq 0.68$ and $-1.91 \leq N_\sigma \leq 1.46$ for signed N_σ. For the absolute case $|N_\sigma| \leq 0.81$ and $|N_\sigma| \leq 1.54$ for 68.3% and 95.4% of the measurements respectively. Alternatively, 82.2% and 98.0% of the measurements fall within $N_\sigma \leq 1$ and $N_\sigma \leq 2$, respectively. The widened tails (narrowness) of the weighted mean (median) distribution is still present.

Similar distributions are found for the RR Lyrae tracer type sub-sample. For weighted mean statistics a central estimate of $(m - M)_0 = 18.86 \pm 5.20 \times 10^{-3}$ mag is found. 68.3% and 95.4% of the measurements are within $-2.40 \leq N_\sigma \leq 0.88$ and $-2.40 \leq N_\sigma \leq 1.47$ for

signed N_σ.[17] For the absolute case, $|N_\sigma| \leq 1.49$ and $|N_\sigma| \leq 3.26$ for 68.3% and 95.4% of the measurements respectively. 50.0% and 80.0% of the measurements fall within $N_\sigma \leq 1$ and $N_\sigma \leq 2$, respectively. For the median case a central estimate of $(m - M)_0 = 18.90$ mag with a 1σ range of 18.74 mag $\leq (m - M)_0 \leq 19.06$ mag is found. The distribution shows that 68.3% and 95.4% of the measurements are within $-0.51 \leq N_\sigma \leq 0.86$ and $-1.13 \leq N_\sigma \leq 1.24$ for signed N_σ. For the absolute case $|N_\sigma| \leq 0.65$ and $|N_\sigma| \leq 1.28$ for 68.3% and 95.4% of the measurements respectively. Alternatively, 83.3% and 100% of the measurements fall within $N_\sigma \leq 1$ and $N_\sigma \leq 2$, respectively.

The distributions are also fit to the four well-known distributions using the KS test. All measurement sets are best fit by a Student's t distribution. The full dataset of 247 measurements is poorly fit by all distributions with a probabilities $< 0.1\%$. However, the RR Lyrae sub-sample is best fit by the double exponential distribution with a probability of 36%. All of the probabilities are listed in Table 3.3.

Table 3.3: *K-S Test Probabilities for SMC Distance Moduli Measurements*

Function[a]	Data Set	Un-binned Probability(%)[b]	Binned Probability(%)[b]
Gaussian	Whole (247)	< 0.1	< 0.1
	Cepheids (101)	< 0.1	< 0.1
	RR Lyrae (30)	8.4	20
Cauchy	Whole (247)	< 0.1	< 0.1
	Cepheids (101)	< 0.1	< 0.1
	RR Lyrae (30)	33	15
Double Exponential	Whole(247)	< 0.1	< 0.1
	Cepheids (101)	< 0.1	< 0.1
	RR Lyrae (30)	36	20
$n = 1$ Student's t	Whole (247)	< 0.1	< 0.1
$n = 1$ Student's t	Cepheids (101)	< 0.1	< 0.1
$n = 57$ Student's t	RR Lyrae (30)	34	17

[a] For the Student's t case, the n corresponding with the best probability is displayed.
[b] The probability that the data set is compatible with the assumed distribution.

[17] The two lower bounds are the same due to the distribution being weighted towards the positive N_σ side (there are more values with $N_\sigma > 0$). Symmetrizing this distribution gives a clearer understanding of the error.

3.6 Conclusions

Using 232 LMC distance moduli measurements from [2], error distributions are constructed in order to examine the possible publication bias and/or correlations between measurements suggested by [2]. The error distributions are found to have wider tails than expected for a Gaussian distribution when using a weighted mean central estimate. Because the weighted mean makes use of an individual measurement's quoted error, this could possibly be a consequence of unaccounted-for systematic errors. In fact, 53 of the 237 measurements compiled by [2] quote a non-zero systematic error. Due to the non-Gaussianity of this error distribution, it is more appropriate to use the median statistics error distribution.

The median statistics error distributions are narrower than expected for a Gaussian distribution. This supports the suggestion of correlations between some measurements, with publication bias possibly contributing mildly.

Chapter 4

Conclusion

As datasets may not always be assumed Gaussian, it is useful to perform statistical tests on measurements to justify such a claim. This can be done by constructing and performing Gaussianity tests on error distributions of measurements. In this thesis, these distributions are constructed by the finding the number of standard deviations that a measurement deviates from a central estimate, either weighted mean or median. Gaussian tests are then done using either a χ^2 analysis or a non-parametric Kolmogorov-Smirnov test to fit the measurements to four well-known distributions: Gaussian, Lorentzian, Student's t, and double exponential.

This thesis first implements this analysis to a ^{7}Li abundance measurement compilation from [1]. The error distribution constructed from these measurements is non-Gaussian with large probability in the tails, and is best fit by an $n = 8$ Student's t distribution.[1] When non-Gaussianity is accounted for, there is a 4.9σ discrepancy between the median A(Li)= 2.21 found from this analysis and the predicted value from *Planck*, A(Li)= 2.69. While this is smaller than the discrepancy of 6.5σ found from assuming Gaussianity, it does not fully resolve the Li problem. However, with more higher-quality measurements, better conclusions may be drawn.

[1] However, this may not hold much physical significance.

Gaussianity tests are also performed on a set of LMC distance moduli measurements. When using the weighted mean as a central estimate, the constructed error distributions are wide as compared to a Gaussian (with large probabilities in the tails). This may be due to unaccounted-for systematic errors, as only 53 of the 237 values from [2] quote a non-zero systematic error. For the median case, the error distributions are narrower than a Gaussian, which may be the consequence of correlations between measurements and/or possible mild publication bias suggested by [2].

Bibliography

[1] M. Spite, F. Spite, and P. Bonifacio. The Cosmic Lithium Problem: An Observer's Perspective. *Mem. S.A.It. Suppl.*, 22:9, 2012.

[2] R. de Grijs, J. E. Wicker, and G. Bono. Clustering of Local Group Distances: Publication Bias or Correlated Measurements? I. The Large Magellanic Cloud. *Astron. J.*, 147:122, 2014.

[3] S. Podariu, T. Souradeep, J. R. Gott, B. Ratra, and M. S. Vogeley. Binned Cosmic Microwave Background Anisotropy Power Spectra: Peak Location. *Astrophys. J.*, 559: 9, 2001.

[4] J. R. Gott, M. S. Vogeley, S. Podariu, and B. Ratra. Median Statistics, H_0, and the Accelerating Universe. *Astrophys. J.*, 549:1, 2001.

[5] G. Chen and B. Ratra. Median Statistics and the Mass Density of the Universe. *Publ. Astron. Soc. Pac.*, 115:1143, 2003.

[6] J. A. Hodge, R. H. Becker, R. L. White, and W. H. de Vries. Radio Detection of Radio-Quiet Galaxies. *Astron. J.*, 136:1097, 2008.

[7] E. E. Mamajek and L. A. Hillenbrand. Improved Age Estimation for Solar-Type Dwarfs Using Activity-Rotation Diagnostics. *Astrophys. J.*, 687:1264, 2008.

[8] N. Bourne, L. Dunne, R. J. Ivison, S. J. Maddox, M. Dickinson, and D. T. Frayer. Evolution of the Far-Infrared-Radio Correlation and Infrared Spectral Energy Distributions of Massive Galaxies over $z = 0 - 2$. *Mon. Not. R. Astron. Soc.*, 410:1155, 2011.

[9] A. Shafieloo, T. Clifton, and P. Ferreira. The Crossing Statistic: Dealing with Unknown Errors in Dispersion of Type Ia Supernovae. *J. Cosmol. Astropart. Phys.*, 1108:017, 2011.

[10] R. A. C. Croft and M. Dailey. On the Measurement of Cosmological Parameters. *Quart. Phys. Rev*, 1:1, 2015.

[11] S. Andreon and M. A. Hurn. Measurement Errors and Scaling Relations in Astrophysics: a Review, arXiv:1210.6232, 2012.

[12] O. Farooq, S. Crandall, and B. Ratra. Binned Hubble Parameter Measurements and the Cosmological Deceleration-Acceleration Transition. *Phys. Lett. B*, 726:72, 2013.

[13] S. Crandall and B. Ratra. Median Statistics Cosmological Parameter Values. *Phys. Lett. B*, 732:330, 2014.

[14] G. Chen and B. Ratra. Median Statistics and the Hubble Constant. *Publ. Astron. Soc. Pac.*, 123:1127, 2011.

[15] E. Calabrese, M. Archidiacono, A. Melchiorri, and B. Ratra. Impact of H_0 Prior on the Evidence for Dark Ratdiation. *Phys. Rev. D*, 86:043520, 2012.

[16] X. Ding, M. Biesiada, S. Cao, Z. Li, and Z. H. Zhu. Is There Evidence for Dark Energy Evolution. *Astrophys. J. Lett.*, 803:L22, 2015.

[17] W. N. Colley and J. R. Gott III. Genus Topology and Cross-Correlation of BICEP2 and Planck 353 GHz B-modes: Further Evidence Favouring Gravity Wave Detection. *Mon. Not. R. Astron. Soc.*, 447:2034, 2015.

[18] M. Sereno. CoMaLit - III. Literature Catalogues of Weak Lensing Clusters of Galaxies (LC^2). *Mon. Not. R. Astron. Soc.*, 450:3665, 2015.

[19] K. Ganga, B. Ratra, J. O. Gundersen, and N. Sugiyama. UCSB South Pole 1994 Cosmic Microwave Background Anisotropy Measurement Constraints on Open and Flat Λ Cold Dark Matter Cosmgonies. *Astrophys. J.*, 484:7, 1997.

[20] B. Ratra, R. Stompor, K. Ganga, G. Rocha, and et al. N. Sugiyama. Cosmic Microwave Background Anisotropy Constraints on Open and Flat Λ Cold Dark Matter Cosmogonies from UCSB South Pole, ARGO, MAX, White Dish, and SuZIE Data. *Astrophys. J.*, 517:549, 1999.

[21] G. Chen, P. Mukherjee, T. Kahniashvili, B. Ratra, and Y. Wang. Looking for Cosmological Alfvén Waves in Wilkinson Microwave Anisotropy Probe Data. *Astrophys. J.*, 611:655, 2004.

[22] C. L. Bennett, D. Larson, J. L. Weiland, N. Jarosik, and et al. G. Hinshaw. Nine-Year Wilkinson Microwave Anisotropy Probe (WMAP) Observations: Final Maps and Results. *Astrophys. J. Suppl. Ser.*, 208:20, 2013.

[23] C. G. Park, C. Park, B. Ratra, and M. Tegmark. Gaussianity of Degree-Scale Cosmic Microwave Background Anisotropy Observations. *Astrophys. J.*, 556:582, 2001.

[24] P. A. R. Ade, N. Aghanim, C. Armitage-Caplan, M. Arnaud, and et al. M. Ashdown. Planck 2013 Results. XXIV. Constraints on Primordial Non-Gaussianity. *Astron. Astrophys.*, 571:A24, 2014.

[25] G. Chen, R. Gott, and B. Ratra. Non-Gaussian Error Distribution of Hubble Constant Measurements. *Publ. Astron. Soc. Pac.*, 115:1269, 2003.

[26] M. Abramowitz and I. A. Stegun. *Handbook of Mathematical Functions*. Dover Publications, 1965.

[27] E. D. Feigelson and G. J. Babu. *Modern Statistical Methods for Astronomy with R Applications*. Cambridge Univ. Press, 2012.

[28] S. Crandall, S. Houston, and B. Ratra. Non-Gaussian Error Distribution of ^{7}Li Abundance Measurements. *Mod. Phys. Lett. A*, 30:25, 2015.

[29] G. Hinshaw, D. Larson, E. Komatsu, D. N. Spergel, and et al. C. L. Bennett. Nine-Year Wilkinson Microwave Anisotropy Probe (WMAP) Observations: Cosmological Parameter Results. *Astrophys. J. Suppl. Ser.*, 208:19, 2013.

[30] P. A. R. Ade, N. Aghanim, M. Arnaud, M. Ashdown, J. Aumont, and et al. Planck 2015 Results. XIII. Cosmological Parameters, arXiv:1502.01589v2, 2015.

[31] K. Jedamzik and M. Pospelov. Big Bang Nucleosynthesis and Particle Dark Matter. *New J. Phys.*, 11:105028, 2009.

[32] M. Spite and F. Spite. *Light Elements of the Universe, eds. C. Charbonnel, M. Tosi, F. Primas and C. Chiappini*, page 201.

[33] G. Steigman. Primordial Nucleosynthesis: The Predicted and Observed Abundances and Their Consequences, arxiv:1008.4765v2, 2010.

[34] B. D. Fields. The Primordial Lithium Problem. *Annu. Rev. Nucl. Part. Sci.*, 61:47, 2011.

[35] A. Frebel and J. E. Norris. *Metal-Poor Stars and the Chemical Enrichment of the Universe*, pages 55–14.

[36] A. Coc, J. P. Uzan, and E. Vangioni. Standard Big Bang Nucleosynthesis and Primordial CNO Abundances After Planck. *J. Cosmol. Astropart. Phys.*, 1410:50, 2014.

[37] J. Meléndez and I. Ramírez. Reappraising the Spite Lithium Plateau: Extremely Thin and Marginally Consistent with WMAP Data. *Astron. J.*, 615:L33, 2004.

[38] J. Meléndez, L. Casagrande, I. Ramírez, M. Asplund, and W. J. Schuster. Observational Evidence for a Broken Li Spite Plateau and Mass-Dependent Li Depletion. *Astron. Astrophys.*, 515:L3, 2010.

[39] J. C. Howk, N. Lehner, B. D. Fields, and G. J. Mathews. Observation of Interstellar Lithium in the Low-Metallicity Small Magellanic Cloud. 489:121, 2012.

[40] K. Jedamzik, K-Y. Choi, L. Roszkowski, and R. R. de Austri. Solving the Cosmic Lithium Problems with Gravitino Dark Matter in the Constrained Minimal Supersymmetric Standard Model. *J. Cosmol. Astropart. Phys.*, 0607:007, 2006.

[41] A. Coc, N. J. Nunes, K. A. Olive, J. P. Uzan, and E. Vangioni. Coupled Variations of Fundamental Couplings and Primordial Nucleosynthesis. 76:023511, 2007.

[42] N. Chakraborty, B. D. Fields, and K. A. Olive. Resonant Destruction as a Possible Solution to the Cosmological Lithium Problem. *Phys. Rev. D*, 83:063006, 2011.

[43] O. Erken, P. Sikivie, H. Tam, and Q. Yang. Axion Dark Matter and Cosmological Parameters. *Phys. Rev. Lett.*, 108:061304, 2012.

[44] R. H. Cyburt, J. Ellis, B. D. Fields, F. Luo, K. A. Olive, and V. C. Spanos. Metastable Charged Sparticles and the Cosmological ^{7}Li Problem. *Phys. Rev. D*, 83:063006, 2011.

[45] R. Ouyed. A Resolution of the Cosmic Lithium Problem, arXiv:1304.3715v2, 2014.

[46] M. Kusakabe and M. Kawasaki. Chemical Separation of Primordial Li^+ During Structure Formation Caused by Nanogauss Magnetic Field. *Mon. Not. R. Astron. Soc.*, 446: 1597, 2015.

[47] P. Bonifacio, P. Molaro, T. Sivarani, R. Cayrel, M. Spite, and et al. First Stars VII - Lithium in Extremely Metal Poor Dwarfs. *Astron. Astrophys.*, 462:851, 2007.

[48] C. Charbonnel and F. Primas. The Lithium Content of the Galactic Halo Stars. *Astron. Astrophys.*, 442:961, 2005.

[49] W. Aoki, P. S. Barklem, T. C. Beers, N. Christlieb, S. Inoue, and et al. Lithium Abundances of Extremely Metal-Poor Turnoff Stars. *Astrophys. J.*, 698:1803, 2009.

[50] A. Hosford, S. G. Ryan, A. E. García Pérez, and K. A. Olive. Lithium Abundances of Halo Dwarfs Based on Excitation Temperature - I. Local Thermodynamic Equilibrium. *Astron. Astrophys.*, 493:601, 2009.

[51] L. Sbordone, P. Bonifacio, E. Caffau, H. G. Ludwig, N. T. Behara, and et al. The Metal-Poor End of the Spite Plateau - I. Stellar Parameters, Metallicities and Lithium Abundances. *Astron. Astrophys.*, 522:A26, 2010.

[52] M. Schaeuble and J. R. King. New Lithium Measurements in Metal-Poor Stars. *Publ. Astron. Soc. Pac.*, 124:164, 2012.

[53] S. Crandall and B. Ratra. Non-Gaussian Error Distributions of LMC Distance Moduli Measurements. *Astrophys. J.*, 815:87, 2015.

[54] B. E. Schaefer. A Problem With the Clustering of Recent Measures of the Distance to the Large Magellanic Cloud. *Astron. J.*, 135:112, 2008.

[55] W. L. Freedman, B. F. Madore, B. K. Gibson, L. Ferrarese, D. D. Kelson, and et al. Final Results from the *Hubble Space Telescope* Key Project to Measure the Hubble Constant. *Astrophys. J.*, 553:47, 2001.

[56] G. Pietrzyński, D. Graczyk, W. Gieren, I. B. Thompson, B. Pilecki, and et al. An Eclipsing-Binary Distance to the Large Magellanic Cloud Accurate to Two Per Cent. 495:76, 2013.

[57] R. de Grijs and G. Bono. Clustering of Local Group Distances: Publication Bias or Correlated Measurements? III. The Small Magellanic Cloud. *Astron. J.*, 149:179, 2015.

Appendix A

A(Li) Error Distribution With an Optimistic $\sigma = 0.06$

[47] argue that the error given by the effective temperature, T_{eff}, is larger than previously thought, and can dominate the overall error of A(Li) measurements. This would result in a constant error for all measurements. An attempt is made to illustrate this effect by repeating the analysis done in Chapter 2 with an optimistic error of $\sigma = 0.06$.[1] Histograms of these error distributions are given in A.1 for both the weighted mean and median cases.

For the weighted mean case, 68.3% of the signed error distribution falls within $-1.48 \leq N_\sigma \leq 0.80$, while 95.4% lies in the range of $-2.47 \leq N_\sigma \leq 1.39$. The absolute magnitude of the error distribution have corresponding limits of $|N_\sigma| \leq 1.15$ and $|N_\sigma| \leq 2.13$. For the median statistics central estimate, 68.3% of the signed error distribution falls within $-1.37 \leq N_\sigma \leq 0.83$, while 95.4% lies within $-2.39 \leq N_\sigma \leq 1.60$. The corresponding absolute magnitude limits are $|N_\sigma| \leq 1.16$ and $|N_\sigma| \leq 2.32$. Alternatively, 62.7% & 94.7% and 65.3% & 95.4% of the data falls within the $|N_\sigma| = 1$ and 2 ranges for the weighted mean and median cases respectively. These values hint at a slightly more Gaussian distribution

[1] The same analysis was done with a larger error of $\sigma = 0.09$ given from [47], and similar conclusions were reached.

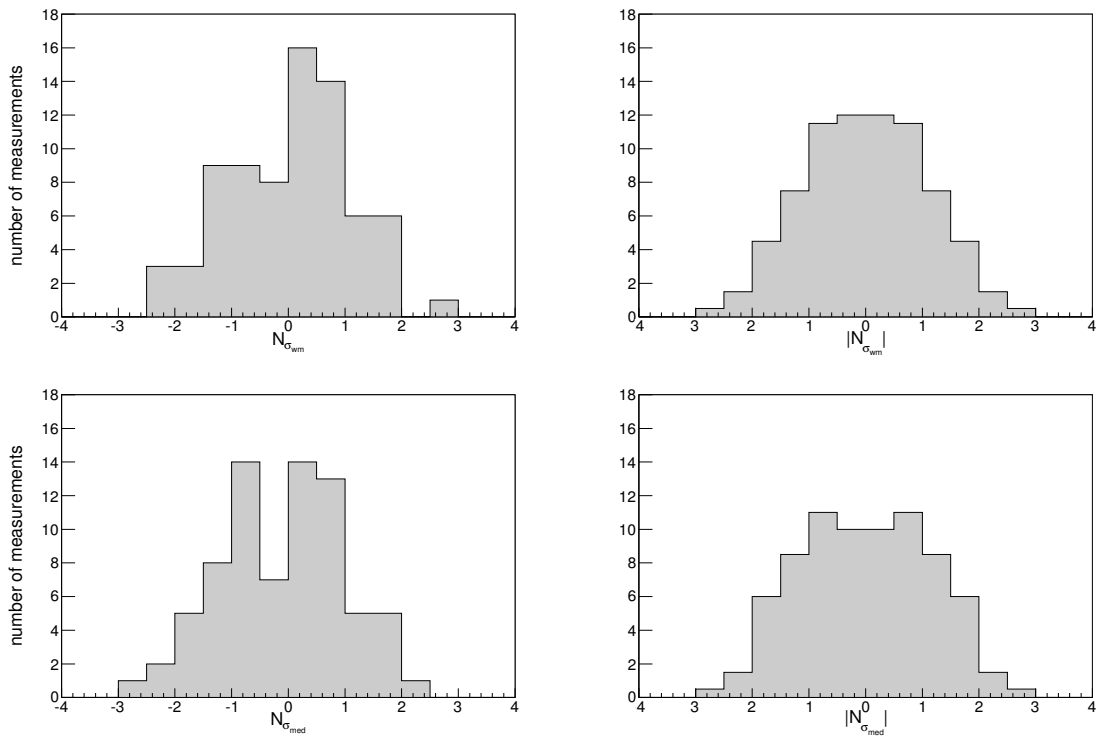

Figure A.1: *Histograms of the error distribution with* $\sigma = 0.06$ *A(Li) values in half standard deviation bins. The top (bottom) plot uses the weighted mean (median) central estimate for* N_σ*. The left and right plots are the signed and absolute, or symmetric, distributions respectively.*

than that from Chapter 2.